Università degli Studi di Modena e Reggio Emilia in convenzione con l'Università degli studi di Parma

CORSO DI DOTTORATO IN NEUROSCIENZE

CICLO XXXII

Sensory and motor properties of physiologically identified neuronal classes in multiple areas of the parieto-frontal grasping network

Relatore:

Prof. Luca Bonini

Coordinatore del Corso di Dottorato:

Prof. Michele Zoli

Candidato:

Carolina Giulia Ferroni

TABLE OF CONTENTS

1. Abstract (english)

The neural machinery underlying sensory and motor processes in the primate brain remain largely unclear. Decades of neurophysiological literature evidenced the presence of distinct neuronal properties in many nodes of the cortical grasping network, from purely motor neurons encoding motor goals to sensorimotor neurons responsive to visually presented objects, observed actions or both. The attribution of these functional properties to specific neuronal classes, such as inhibitory interneurons or pyramidal neurons, would be crucial to achieve a better understanding of the motor-based perceptual and cognitive functions stemming from the inner organization of the motor system. To date, several studies showed that cortical neurons can be identified by jointly considering a variety of features of their spike waveform and firing properties, but the specific relation between physiologically characterized neuronal classes and their coding properties remains unclear, especially in areas of the primates' motor system.

To address this issue, here we studied the features of extracellularly recorded spikes of 355 well-isolated single neurons. Neurons were sampled from 5 hemispheres of 3 macaque monkeys while they performed or observed an experimenter performing, a reaching-grasping go/no-go task with three different objects as targets. Single neuron activity was recorded from anterior intraparietal area AIP (n=86), ventral premotor area F5 (n=106) and pre-supplementary motor area F6 (n=163). First, we performed an unsupervised clustering of spike waveforms that reliably dissociated 3 clusters. We found that physiologically-identified classes of cells, unevenly distributed across the investigated areas, carry distinct visuomotor signals. Broadly spiking neurons are prevalent in area F6 and exhibit a balanced amount of facilitated and suppressed activity during action execution and observation. In contrast, narrow spiking neurons are mostly facilitated by visual signals and show greater mutual modulation of their motor and visual response during one's own and others' action, particularly in areas AIP and F5.

These findings shed light on the cellular mechanisms underlying local processing of sensorimotor information for planning and executing grasping actions and for processing

others' observed action. Further studies may unravel the contribution of larger cortico-subcortical brain network to the mechanisms elucidated by the present work.

2. Abstract (italiano)

I meccanismi neurali che sottendono i processi sensoriali e motori nel cervello dei primati non sono ancora stati chiariti. Decenni di letteratura neurofisiologica evidenziano la presenza di distinte proprietà neuronali in molti nodi dei circuiti corticali per l'afferramento, dai neuroni puramente motori che codificano lo scopo a quelli sensori-motori che rispondono alla presentazione visiva di oggetti, azioni o entrambi. L'attribuzione di queste proprietà funzionali a specifiche classi neuronali, come agli interneuroni inibitori o ai neuroni piramidali, sarebbe fondamentale per comprendere al meglio le funzioni cognitive e percettive che emergono dalla organizzazione intrinseca del sistema motorio. Ad oggi, molti studi mostrano che i neuroni corticali possono essere identificati prendendo in considerazione le diverse caratteristiche della loro forma d'onda e delle loro proprietà di scarica. Tuttavia, la specifica relazione tra classi neuronali identificate fisiologicamente e le loro proprietà di codifica resta ancora da chiarire, specialmente nelle aree appartenenti al sistema motorio dei primati.

Per indagare questo problema abbiamo studiato le caratteristiche dei potenziali d'azione di 355 singoli neuroni ben isolati registrati extracellularmente. I neuroni sono stati registrati in 5 emisferi di tre scimmie macaco mentre svolgevano un compito di raggiungimento e afferramento di tipo go/nogo con tre differenti oggetti bersaglio, e mentre osservavano uno sperimentatore svolgere lo stesso compito. L'attività dei singoli neuroni è stata registrata dall'area intraparietale anteriore AIP (n=86), dall'area premotoria ventrale F5 (n=106) e dall'area pre-supplementare motoria F6 (n=163). Inizialmente abbiamo suddiviso tutte le forme d'onda registrate nelle tre aree in 3 gruppi attraverso una procedura di clustering non supervisionato. Queste tre classi di neuroni presentavano caratteristiche fisiologiche diverse e non si distribuivano uniformemente tra le aree. Nell' area F6 prevalevano cellule con forma d'onda ampia e il numero di neuroni facilitati e inibiti era bilanciato sia durante il compito di esecuzione sia durante quello di osservazione. Al contrario, i neuroni con forma d'onda stretta risultavano più facilitati dai segnali visivi e dotati di una maggiore modulazione visuo-motoria congiunta sia quando l'azione veniva compiuta sia quando veniva osservata, soprattutto nelle are AIP e F5.

Questi risultati chiariscono i meccanismi cellulari alla base dell'elaborazione locale delle informazioni sensori-motorie per la pianificazione, l'esecuzione e l'osservazione di azioni di prensione. Ulteriori studi potrebbero rilevare il contributo di reti cortico-sottocorticali più ampie ai meccanismi chiariti nel presente lavoro.

3. Introduction

3.1 The cortical grasping network

Grasping is one of the most important motor acts that primates perform in their everyday life for interacting with different objects in different ways (Cisek and Kalaska 2010). The primary mechanism allowing primates to grasp visually presented objects is the transformation of their sensory properties into appropriate motor plans to control the hand (Schaffelhofer and Scherberger 2016).

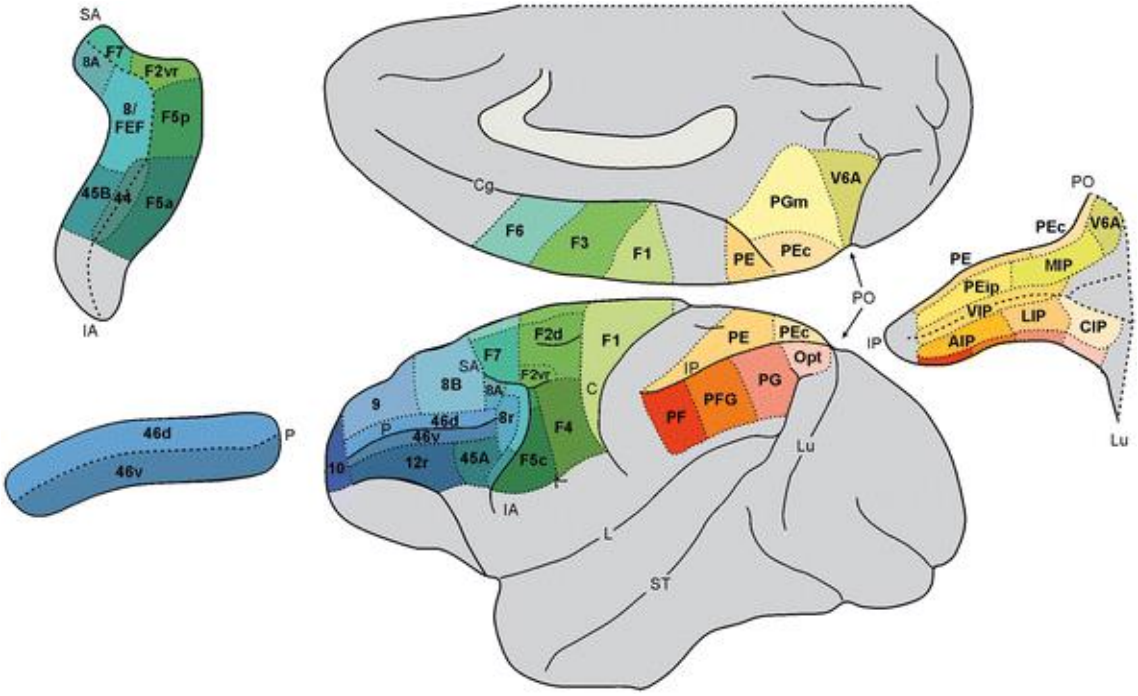

Figure 1. Cytoarchitectonic parcellation of the extended parieto-frontal motor system in the macaque. The prefrontal cortex is subdivided according to Carmichael and Price (1994), the caudo-ventral part of prefrontal cortex according to Gerbella et al (2007). Agranular frontal cortex is subdivided according to Matelli et al. 1991 and Belmalih et al. (2008). Parietal areas are classified according to Pandya and Seltzer 1982. Modified by Gerbella et al. (2017).

Classically, the cortical areas (Figure 1) most directly involved in object-grasping were deemed to be the anterior part of the intraparietal lobule (Gardner et al. 2007), namely area AIP (Sakata et al. 1995), and the ventral premotor area F5 (Murata et al. 1997; Jeannerod et al. 1995). Reversible inactivation of either the parietal (Gallese et al.

1994) or premotor (Fogassi et al. 2001) nodes of this circuit produces impairments in the visually guided grasping of objects. More recent neurophysiological studies also added to this circuit the posterior parietal area V6A (Fattori et al. 2010) and the dorsal premotor area F2 (Raos et al. 2006), as well as the mesial presupplementary motor area F6 (Lanzilotto et al. 2016), thus forming a larger and reciprocally interconnected system of areas underlying the processing of objects for grasping them (Gerbella et al. 2017; Borra et al. 2017).

Interestingly, since the seminal papers on the so-called "mirror neurons" (di Pellegrino et al. 1992; Gallese et al. 1996; Giacomo Rizzolatti et al. 1996), it became more and more clear that the areas underlying grasping execution also play a role in the encoding of similar manual actions performed by others. Indeed, mirror neurons discharge during both the execution and observation of an action performed by another individual, but also show remarkable generative capacity by signalling 1) partially occluded actions (in which the critical phase of hand-object interaction is hidden, see (Umiltà et al. 2001) 2) completely invisible noisy actions based on their sound (Kohler et al. 2002), 3) forthcoming stages of natural action sequences (Fogassi et al. 2005; Bonini et al. 2009) or contextually triggered actions of others (Maranesi et al. 2015; Mazurek et al. 2018) and 4) internally generated neural representations of others' withheld actions (Bonini et al. 2014b).

These neuronal properties have been found in a larger network of anatomically connected brain regions (Nelissen et al. 2011; Bruni et al. 2018; Albertini et al. 2020; Lanzilotto et al. 2019), largely exceeding area F5 where mirror neurons were originally discovered. These areas form a so-called action observation network (AON), which extensively overlap with the extended cortical grasping network. Although the ventral premotor area F5 is thought to be the core of the AON and is certainly the most widely studied region in the mirror neuron literature (Kilner and Lemon 2013; Bonini 2017), two other areas included in the cortical grasping network recently gained increasing interest in the AON as well: the anterior intraparietal area AIP and the pre-supplementary motor area F6.

Area AIP neurons discharge during the observation of other's action, often combining visual and motor representation of actions (Maeda et al. 2015; Pani et al. 2014). Recently, AIP has been proposed as a main hub in the AON (Lanzilotto et al. 2019) because of its role in routing to F5 visual information regarding manipulative actions of others. Most importantly, AIP shows considerable selectivity for observed actions against

other visual stimuli, exhibiting the remarkable capacity to provide some form of visual-invariant representation of specific manipulative action exemplars (Marco Lanzilotto et al. 2020). Concerning area F6, it has been subject to mounting interest because it hosts neurons selectively encoding the action of others (Yoshida et al. 2011). Although similar neurons were also found in area F5 (Gallese et al. 1996) and AIP (Maeda et al. 2015), recent studies showed that F6 can even predict other's intended actions by encoding visually presented objects selectively when they are targeted by one's own or another agent's action, or both, thus "mirroring" objects in addition to actions (Livi et al. 2019) by virtue of its strong link with both prefrontal and premotor areas (Albertini et al. 2020).

In the following sections, I will first review the existing evidence about the cortical mechanisms underlying object grasping in these three main cortical nodes. Then, I will show their tuning specificities regarding the representation of manual actions of others. Finally, I will highlight the surprisingly poor evidence in this literature about the possible local cell-type mechanisms underlying system-level interactions between these areas during the processing of objects and the execution of grasping action of self and others.

3.1.1 Visuomotor processing of objects in parietal and premotor cortex

The anterior intraparietal area (AIP)

Area AIP is located in the anterior part of the intraparietal sulcus and, classically, it is deemed to host different types of neurons related to the visual processing of objects: visual dominant and visuomotor neurons (Murata et al. 2000) (Figure 2). In addition, it also hosts motor dominant neurons, which respond with possible object/grip type specificity only during the grasping movement, even in the dark, while remaining silent during object fixation. Visual dominant neurons discharge only during object fixation and/or during grasping in the light, but not in the dark, thus showing no evidence of truly motor-related activity. In contrast, visuomotor neurons discharge also during grasping in the dark, with possible differential activity relative to grasping in the light, and/or during object fixation (Murata et al. 2000; Sakata et al. 1995; Taira et al. 1990), thus showing both visual and motor activity.

More recent findings (Schaffelhofer and Scherberger 2016) have shown that AIP neurons have a leading role in extracting from the visual features of an object the most relevant signal to contribute to the premotor planning of grasping actions in area F5. In turn, this latter region drives F1, which ultimately controls the hand for grasping

execution. Noteworthy, reversible inactivation of area AIP has been proved to cause marked impairment in the hand kinematics during visually guided grasping of objects (Gallese et al. 1994), providing causal evidence on the role of this region in the visuomotor transformations.

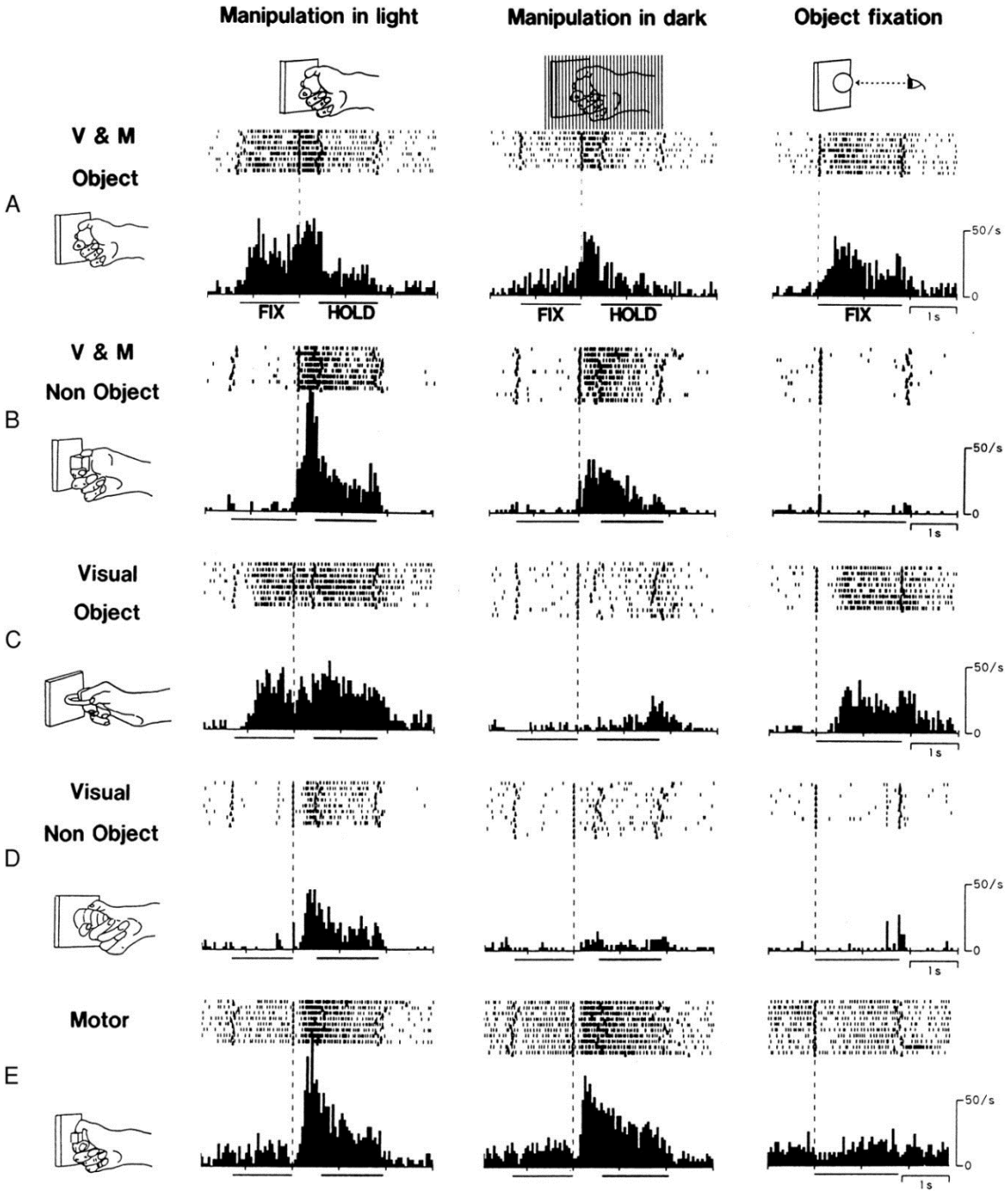

Figure 2. Examples of five different types of AIP hand-manipulation neurons. Each neuron is tested during grasping/manipulation in the light and in the dark, and when the monkey simply fixates the object (from Murata et al. 2000).

The ventral premotor area F5

Area F5 is located in the ventral part of the macaque premotor cortex and is considered a hub of the lateral grasping network. Intracortical microstimulation showed that F5 is involved in the control of hand movement (Hepp-Reymond et al. 1994; Kurata and Tanji 1986; Rizzolatti et al. 1981; Rizzolatti et al. 1988; Maranesi et al. 2012), and the inactivation of the sector of F5 lying in the posterior bank of the inferior arcuate sulcus produces impairments during visually guided grasping (Fogassi et al. 2001b). The neural bases of these effects appear to be represented by two different types of hand-related neurons: purely motor and visuomotor neurons (Rizzolatti et al. 1988; Murata et al. 1997; Raos et al. 2006; Maranesi et al. 2012; Bonini et al. 2014a). Similarly to AIP, F5 purely motor neurons discharge only when the agent executes a specific motor act, in the light as well as in the dark, whereas visuomotor neurons (Figure 3) discharge also during the visual presentation of graspable objects. Visual dominant neurons encoding observed object or one's own action visual feedback with no motor response are deemed to be virtually absent in F5 (although in 1996 Gallese and coworkers reported that approximately 20% of F5 neurons responding to observed action of others did not show any motor response).

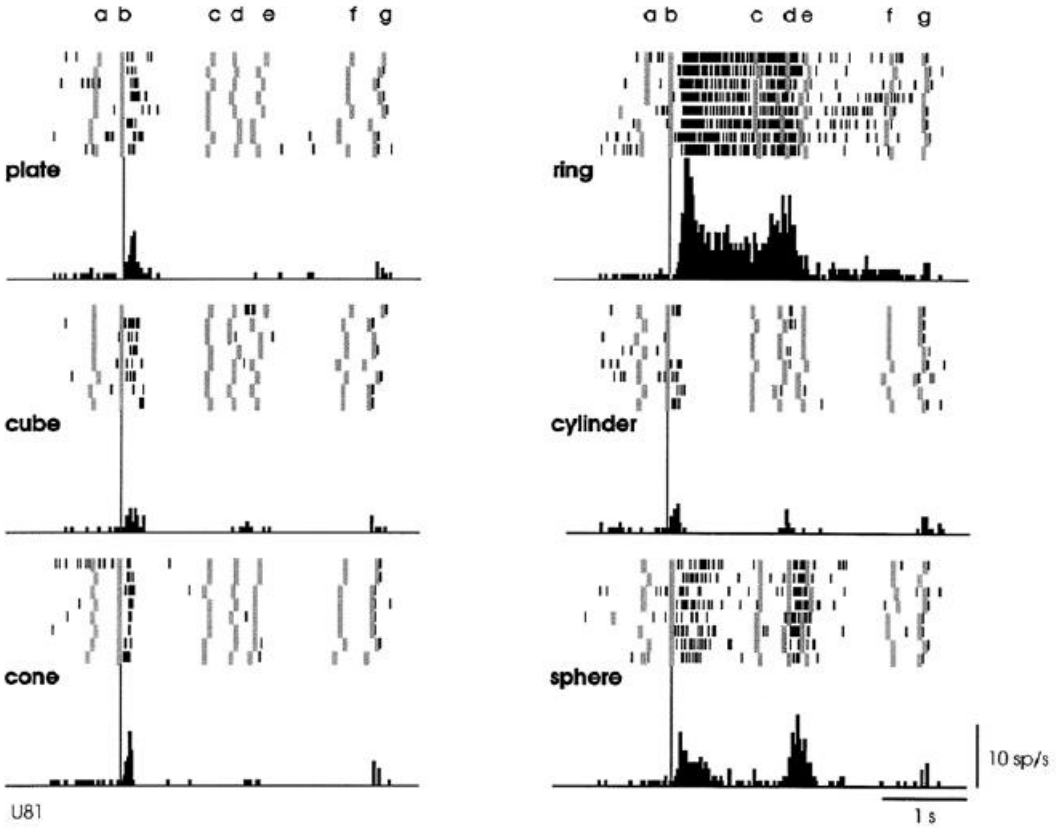

Figure 3. Example of a visuomotor neuron of area F5. This neuron responds both during the visual presentation of the target (first vertical bar, alignment point) and during active grasping (events c, d and e), but with a marked selectivity for the ring object and, to a lesser extent, for the sphere. Letters on top of each plot, corresponding to the grey bars below, indicate: a=onset of red LED (fixation), b= key press (initial position), c= onset of the first green LED (instruction), d=key release, e= onset of object pulling, f= onset of second green LED, g= object release (from Murata et al. 1997).

The pre-supplementary motor area F6

Area F6, lying in the mesial wall of the frontal cortex, is classically deemed to control global actions involving reaching and grasping movements and, in particular, in triggering movement onset, specifying "whether" and "when" an action has to be performed (Rizzolatti et al. 1990). Relative to the lateral premotor areas, in F6 it is generally more difficult to elicit behavioural responses with intracortical microstimulation: only with relatively high current intensity (> 40 μA) and long train durations (> 100 ms) it is possible to evoke forelimbs movements, which appear often slow and complex (Luppino et al. 1991). Nonetheless, wrist and multiple-finger movements have been also observed (Lanzilotto et al. 2016). Area F6 also plays a role in learning and controlling sequential behaviours (Tanji 2001; Nachev et al. 2008).

More recent works (Lanzilotto et al. 2016) studied F6 neurons during a Go/No-go visuo-motor task (VMT) and showed that they can be classified into visuomotor and purely motor (Figure 4 A-D), likewise in previous studies in AIP and F5. Since the same task was previously used to characterize area F5 neurons in the same animals, the direct comparison of the functional proprieties of the two areas allowed to reveal remarkable similarities, supporting the idea of a functional interaction between them, in line with their well-established anatomical connections (Luppino et al. 1991). Nonetheless, the authors also observed some important differences: area F6 motor-related neurons became active and peaked earlier than those of area F5, and visuomotor neurons showed earlier onset and highly transient discharge during visual presentation of the target and, subsequently, during reaching-grasping action with respect to F5 (Figure 4 E-H).

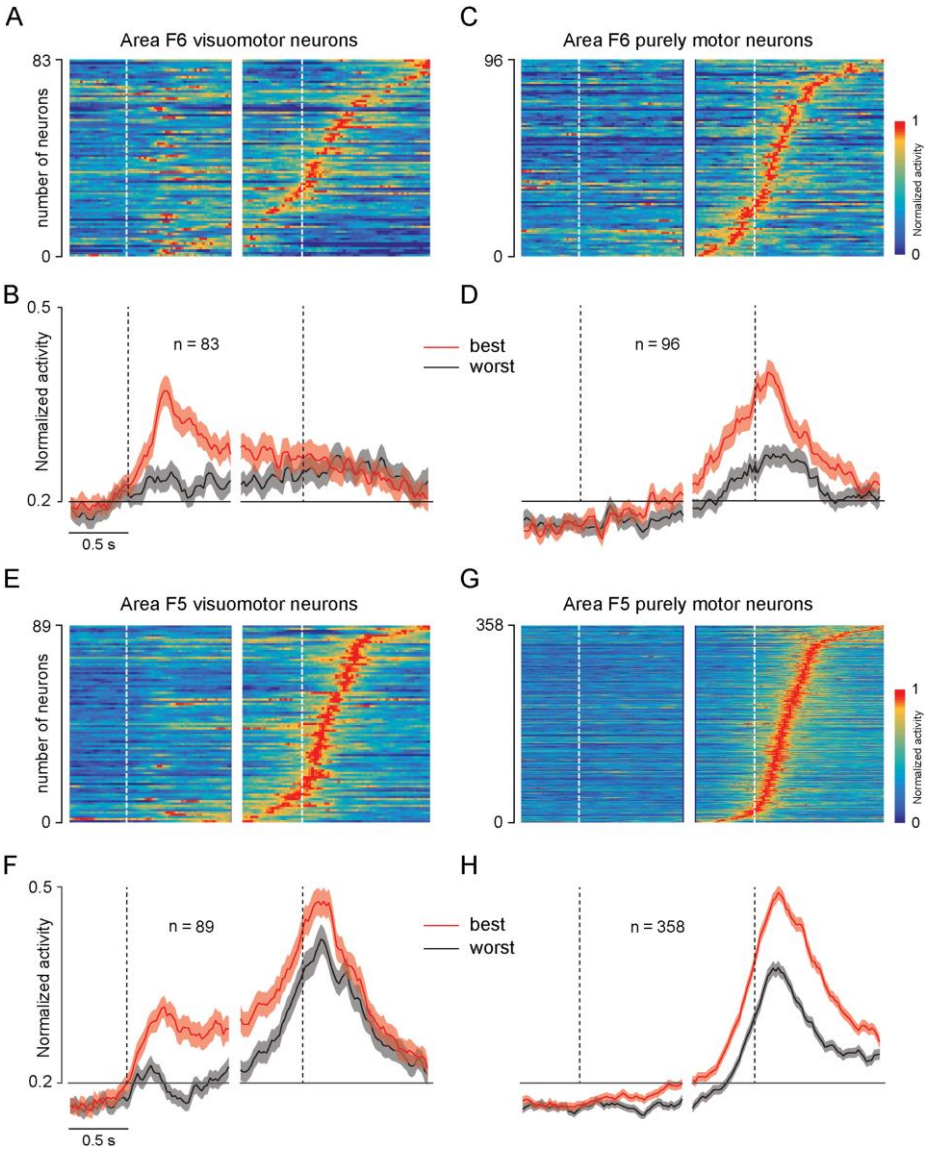

Figure 4. Area F6 visuomotor and motor-related neurons' population response and comparison with the neuronal properties of area F5 (Lanzilotto et al. 2016).

3.1.2 Encoding of actions of self and others in parietal and premotor nodes of the AON

The parietal cortex

Neurons encoding the action of self and others were discovered in the posterior parietal cortex and, specifically, in the inferior parietal area PFG (Gallese et al. 2002; Fogassi et al. 2005; Rozzi et al. 2008), in areas AIP (Pani et al. 201; Maeda et al. 2015; Lanzilotto et al. 2019, 2020), LIP (Shepherd et al. 2009) and V6A (Breveglieri et al. 2019).

Among these areas, AIP is gaining increasing interest in recent years because of its crucial role in linking visual regions of the temporal cortex (Nelissen et al. 2011),

known to host neurons tuned to a multiplicity of visual signals related to others' body parts and bodily actions (Jellema et al. 2000; Jellema and Perrett 2003; Saxe et al. 2004), with the other regions of the AON, particularly F5 (Marco Lanzilotto et al. 2019).

Although only recently studies started to provide direct evidence of neurons with mirror-like properties in AIP (Pani et al. 2014; Maeda et al. 2015), most of these evidence did not include control experiments with relevant stimuli depicting non biological movement and, among action stimuli, focused exclusively on grasping actions. In a recent study we explored a larger variety of natural visual stimuli, depicting videos of individual and social manual actions (like grasping and grooming) as well as a larger variety of biologically relevant stimuli (such as facial or postural displays of other monkeys and non-biological motion stimuli), showing that AIP neurons are particularly tuned to manual actions (Lanzilotto et al. 2020). Importantly, AIP neurons also encode selectively specific manual action exemplars, revealing their additional capacity to keep a stable selectivity despite large visual changes in the presented actions (such as in their viewpoint or the body posture of the filmed actor). Together with the most recent anatomo-functional evidence from our group (Lanzilotto et al. 2019), these findings support the role of AIP as a hub in the AON.

AIP also host neurons called "visual dominant non-object type neurons" (Sakata et al. 1995; Maeda et al. 2015), which fire when the monkey grasps an object in the light but not in the dark. Intriguingly, these neurons do not fire when the object is simply visually presented, with no need for the monkey to perform any action directed to it, hence suggesting that AIP also hosts a set of neurons specifically contributing to the visuomotor processing of monkey's own hand actions.

The ventral premotor cortex

The ventral premotor cortex, in particular area F5, constitutes the first region in which neurons with mirror properties were originally discovered and most extensively described (Kilner and Lemon 2013). Within agranular frontal cortex, accumulating evidence also reported neurons with similar properties in dorsal premotor (Cisek and Kalaska 2004; Papadourakis and Raos 2017) and primary motor (Dushanova and Donoghue 2010; Tkach et al. 2007; Vigneswaran et al. 2013) cortex. Although evidence suggested that the mechanism in the dorsal premotor cortex could be more accurately described as a kind of mental rehearsal (Cisek and Kalaska 2004; Tkach et al. 2007), PMd neurons selective for

the type of observed grip have been shown to have features extremely similar to those of area F5 (Papadourakis and Raos 2017).

The prominent role of F5 in the AON has been also demonstrated by cross-modal multi-voxel patter analysis (MVPA) in fMRI studies of monkeys committed to observe and execute grasping actions. Indeed, Fiave and collegues (2018) found cross-modal representations of action of self and others and, in particular, observed greater cross-modal classification accuracy in area F5 when using motor data for training a classifier and testing its performance on visual data. Furthermore, F5 is also considered a central node in the AON thanks to the direct connections of its spots hosting mirror neurons with the other nodes of the network involved in the processing of observed actions, such as areas AIP/PFG and, indirectly, the areas in the bank of STS (Nelissen et al. 2011; Bruni et al. 2018). The mirror neurons of area F5 are also influenced by the visual perspective from which anothers' action is observed; nonetheless, the presence of view-variant mirror neurons in area F5 is consistent with their role in extracting the overall goal of an observed action, irrespective of the visual details (Caggiano et al. 2011), although the first person perspective appears to retain a particular relevance (Caggiano et al. 2015; Maranesi et al. 2015) even in the adulthood.

The mesial frontal cortex

The mesial frontal cortex is a region that has gained increasing interest since the description of neurons, most frequently found in correspondence of the presupplementary area F6, which selectively encode others' observed action (Yoshida et al. 2011), goals (Falcone et al. 2016) or future choices (Falcone et al. 2017). Besides motor (self) and mirror-type neurons, other-type neurons were deemed to be important in selectively representing information related to others. Similar evidence has been also reported in an homolog region of the human brain, while patients executed and observed hand grasping actions (Mukamel et al. 2010), indicating that the mesial frontal cortex plays a key role in the AON. The relevance of mesial frontal cortex in social monitoring is also supported by the finding, in areas 9 (and 46vr) of a set of neurons that are active during observation of head rotation and discharge also when the monkey rotated its head (Lanzilotto et al. 2017).

In the last few years, the pre-supplementary area F6 has been added as a node of the cortical grasping network (Lanzilotto et al. 2016), but its visuomotor neurons have been shown to display complex agent-based tuning for target objects besides actions.

Indeed, when the monkey viewed a real object as a possible target for its own or another agent's action, F6 neurons could code the visually presented objects when they are targeted by the monkey's own action (self-type), another agent's action (other-type), or both (self- and other-type), as previously shown for actions by Yoshida and coworkers (2011). These findings suggested the existence in area F6 of an "object mirroring" mechanism, which allows observers to predict others' impending action by recruiting the same motor representation they would use for planning their own action in the same context (Livi et al. 2019).

The strong and reciprocal anatomical link of F6 with prefrontal, parietal and premotor regions, which form rostro-caudal gradients overlapped with functional gradients in its neuronal properties (Albertini et al. 2020), highlight the crucial role of this region in orchestrating context-based object processing for self and others' action.

3.2 From system level to local circuitries

An important limitation of the existing literature is that the neural mechanisms and circuits underlying the visuomotor processing of graspable objects and the action of self and others have been so far investigated only at the system level and with a multiplicity of different approaches and tasks in each area. This prevents us from achieving a detailed and comprehensive picture of these mechanisms, from local cell-type specificities (Trainito et al. 2019) to the cortico-cortical circuits (Caminiti et al. 2017).

3.2.1 Classification of neurons based on firing properties.

Besides cortico-cortical connections among distant brain areas, neuronal diversity and the organization of local circuitries are deemed to play a crucial role in mediating the brain-behaviour relationship. However, as compared to system-level mechanisms, the contribution of local circuitries and specific cell types remain elusive, especially in the literature on primates' motor system.

Because of the importance of the issue, in the last two decades several studies looked for a way to characterize cell classes in different areas of the primate cerebral cortex. Of course, the classification of cell types can be based on morphological, molecular or genetic markers, but all these characteristics cannot be used for classifying single neurons isolated in extracellular recordings in vivo. Firing patterns and action-

potential shape can, instead, be a realistic indicator for distinguishing between cell classes in the neocortex.

Morphologically, the neurons can be grossly subdivided into pyramidal cells and GABAergic interneurons: studies *in vitro* demonstrated that these two types of neurons differ in their firing pattern and action-potential shape (McCormick et al. 1985). Furthermore, studies in vivo carried out in mice (Henze et al. 2000) demonstrated that extracellularly recorded features are correlated with intracellular ones. The firing pattern of extracellularly recorded neurons differed across neocortical regions (Maimon and Assad 2009), and intracellular recording studies have used the pattern of discharge for distinguishing different types of functional neurons.

Connors and Gutnick (1990) showed that neurons in the neocortex are not physiologically homogeneous. They described three basic types of neocortical neurons derived mostly from studies of rodents *in vivo* and slices *in vitro*: regular spiking, fast spiking and intrinsically bursting. Regular spiking neurons, originally identified by Mountcastle and colleagues (1969) and called "regular action potentials", most commonly generate only a single spike when stimulated at threshold, and as the stimulus amplitude increases the interspike interval decreases as a function of stimulus intensity. Fast-spiking neurons, characterized by thin spikes, were more rarely encountered by Mountcastle in the monkey cortex, as well as in rat neocortex by Simons and coworkers (1978): these cells show repetitive firing pattern during prolonged intracellular current pulses and are subject to little or no adaptation. When strongly stimulated, they can sustain spike frequencies up to 500-600 Hz for hundreds of milliseconds. Finally, intrinsically bursting neurons show stereotyped, clustered pattern of activity, with the rare tendency to generate clusters of high-frequency spikes, usually limited to certain laminae (Connors and Gutnick 1990).

Several studies tried to identify unique categories of neurons with distinctive anatomical and functional features. Nowak and coworkers (2003) described four major electrophysiologically defined classes of neurons recorded intracellularly from the cat visual area 17: regular spiking, fast spiking, intrinsically bursting and chattering neurons, previously demonstrated also in other works (Connors et al. 1982; Gray and McCormick 1996; McCormick et al. 1985). This study indicated that each group is composed by distinct subclasses, and each of them displays a unique combination of spike shape and spike discharge features. First, neurons can be segregated based of the logarithm of their

inter-spike intervals (ISIs) in two major groups: non-bursting neurons (Figure 5 A-B) and bursting neurons (Figure 5 C-D) based on the bimodal distribution of the log ISIs.

Regular spiking cells (RS) (Fig. 5A) generate tonic trains of action potentials that showed spike frequency adaptation. This class includes pyramidal cells, spiny stellate neurons and some subtypes of local inhibitory interneurons.

Fast spiking cells (FS) (Fig. 5B) respond to depolarizing current pulses with a tonic train of action potentials of relatively short duration. Nowak and coworkers (2003) suggest that this cell may correspond to inhibitory interneurons.

Chattering cells (CH) (Fig.5C) generate repetitive burst of thin (<0.55 ms) action potentials with intra-burst firing rates exceeding 350 Hz. Morphologically, they are pyramidal cells that could be involved in fast transfer of signals between cortical areas.

Intrinsic bursting neurons (IB) (Fig.5D) morphologically are typical pyramidal neurons and electrophysiologically generate a burst of spikes through the activation of an afterdepolarization following each action potential.

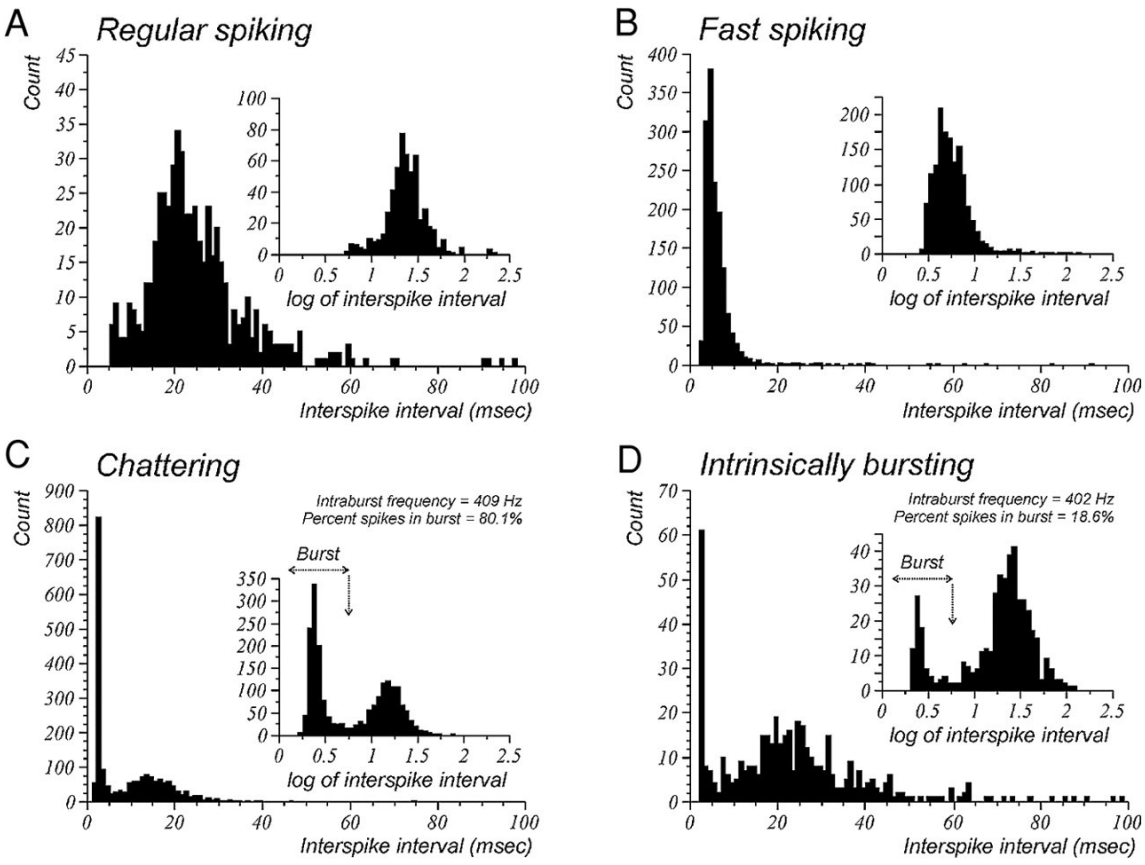

Figure 5. Interspike interval histograms (ISIHs) in bursting (A-B) and nonbursting neurons. (C-D) modified from Nowak et al. 2003

The work by Nowak and coworkers suggest a relatively simple scheme that allows one to classify cells in four major classes based on their ISIs. However, it remains to be clarified whether and to what extent different physiologically-identified cell classes also exhibit distinctive coding properties when studied during specific behavioural tasks in awake behaving animal models (Katai et al. 2010; Cohen et al. 2009). The same classes of neurons identified by Nowak (2003) have been identified by Katai and colleagues (2010) using a cluster analysis based on the NSB (maximum Number of Spikes within a Burst) and the maximum ISI in bursts of extracellularly recorded spikes. The analysis of neurons was focused on those exhibiting task related activity, leading to distinguishing four classes of cells with different characteristic in response to current pulse (Figure 6), as follows.

– **Non-bursting neurons**, which correspond to regular spiking neurons recorded intracellulary, are excitatory neurons and during the task exhibited both excitatory visual response and excitatory pre-saccadic activity.

– **Type I bursting** are inhibitory neurons that shows phasic visual response and pre-saccadic suppressions during the task. This type of neurons can be identified with FS neurons recorded intracellularly.

– **Type II bursting** may be identified with chattering neurons recorded intracellularly; they are excitatory neurons that respond during visual stimuli, show pre saccadic activity and exhibit repetitive burst of activity.

– **Type III bursting** are excitatory neurons that respond during visual stimulation and show pre-saccadic activity, likewise type II bursting, but these neurons have a maximal ISI higher than 5 ms whereas this is lower than 5 ms in Type II. Type III bursting neurons are comparable to intrinsic bursting neurons (IB) recorded intracellularly.

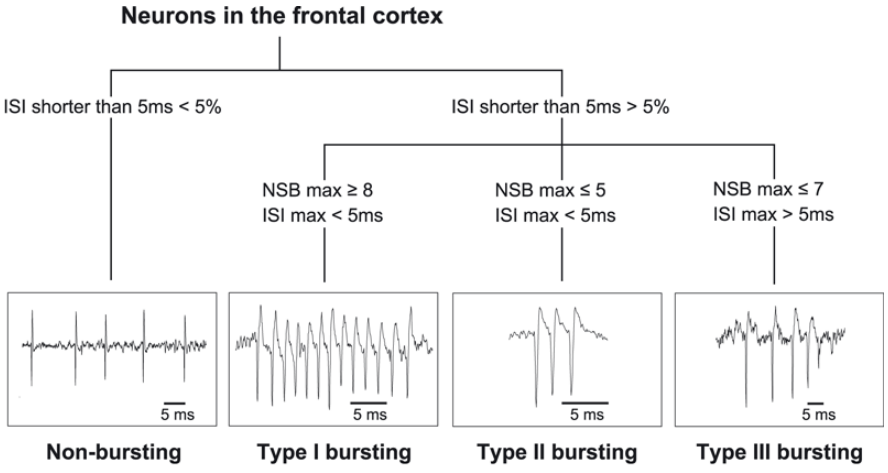

Discharge patterns	Non-bursting	Type I bursting	Type II bursting	Type III bursting
Relation to intracellularly identified neuronay types	RS	FS	FRB (Chattering)	IB
Neuronal interactions	Excitatory	Inhibitory	Excitatory	Excitatory
Task-related activity	Excitatory visual response Excitatory pre-saccadic activity	Phasic visual response Pre-saccadic suppression	Excitatory visual response Excitatory pre-saccadic activity (Repetitive burst discharges)	Excitatory visual response Excitatory pre-saccadic activity

Figure 6. Summary of the firing proprieties of different neurons recorded extracellularly. The classifications of neurons is based on their discharge pattern in frontal cortex. RS= regular spiking, FS=fast spiking, FRB fast rhythmic bursting neurons, IB= intrinsic bursting neurons (Katai et al. 2010).

Studies in vitro showed that FS are GABAergic inhibitory interneurons and have the dendritic morphology and chemical signature of GABAergic cell (McCormick et al. 1985; Schwartzkroin and Kunkel 1985). Extracellular recordings in Rhesus monkeys confirm this hypothesis indirectly like the work of Wilson and colleagues in 1994 (Wilson 1994): during a visual memory-guided oculomotor tasks, they showed that both fast and regular spiking neurons had similar receptive field but FS neurons had high firing rate. These features support the idea that FS cells represent GABAergic inhibitory interneurons.

FS neurons and RS neurons defined according to Mountcastle et al (1969) have been suggested to correspond to interneurons and pyramidal cells, respectively (Rao, Williams, and Goldman-Rakic 1999).

Constantinidis and Goldman-Rakic (2002) applied an ODR task in monkeys and demonstrated that Fast spiking neurons (FS) - putative inhibitory cells - exhibit substantially correlated discharges with respect to regular spiking - putative excitatory neurons. These two types of neurons possess spatially tuned memory fields confirming previous studies (Rao et al 1999; Wilson et al 1994) and FS units were more broadly tuned than RS ones.

In conclusion the extracellular activity reflects intracellular activity, and the different cell classes based on discharge features reflect different physiological properties.

3.2.2 Classification of neurons based on waveform features

Indexes capable to suggest a more direct correspondence between physiological features and morphology of individual cells may be identified in the extracellularly recorded spike waveforms. These have been used to discriminate different subpopulations of cortical neurons in rat (Barthó et al. 2004), cat (Mountcastle et al. 1969), and non-human primates (Chang et al. 2008; Cohen et al. 2009; Mitchell et al. 2007; Song and McPeek 2010). The most distinctive and widely measured features to separate neurons into classes have been the through-to-peak (Trainito et al. 2019), the spike width (Moore and Wehr 2013), the repolarization time (Ardid et al. 2015) and peak to through (Figure 7) (Mitchell et al. 2007; Torres-Gomez et al. 2020).

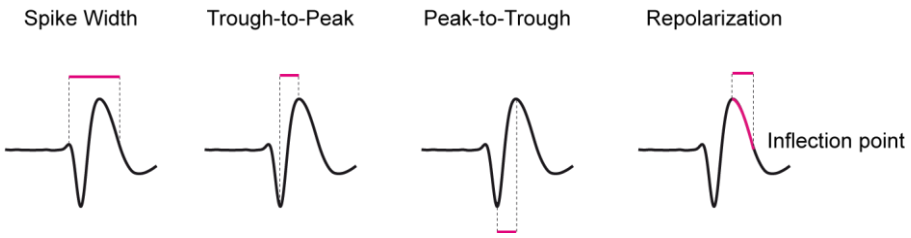

Figure 7. Distinctive spike feature measures to classify neurons into classes: spike width (Moore et al 2013), through-to-peak (Trainito et al. 2019), peak-to-thorugh (Gomez et al. 2020) and repolarization time (Ardid et al. 2015).

A wide variety of experiments in monkey carried out in different cortical areas demonstrated that the classifications based on the spike waveform features is useful for discriminating two main classes of neurons: broad- and narrow spiking. Thanks to histological studies, intracellular and extracellular data analysis, the pyramidal cells typically show broader action potentials than interneurons (Connors and Gutnick 1990; Markram et al. 2004). The pyramidal cells represent approximately the 80% of neocortical cells (Yasuo Kawaguchi et al. 1995; Gabbott and Bacon 1996; Gabbott et al. 1997) whereas interneurons represent the remaining 20% (Wilson 1994; Homayoun and Moghaddam 2007). Interestingly, broad- and narrow spiking neurons show different task-related tuning.

For example, in area V4 of rhesus macaque (Mitchell et al. 2007) neurons classified based on their extracellular action potential (peak to trough) differ in their baseline firing rates and stimulus presentation response during an attention-demanding task, as well as regarding two different measures of attention-dependent response modulation. In particular V4 narrow-spiking neurons exhibited firing rates that were two-fold higher than those of broad-spiking neurons, both in response to a stimulus and during spontaneous firing whit no stimulus in the receptive field. Larger attention-dependent increase in absolute firing rate of narrow-spiking neurons with respect to broad-spiking neurons support the claim that they correspond to functionally distinct cell types.

Additional evidence comes from investigations of the dorsal premotor cortex (PMd). Kaufman and colleagues (2010) subdivided PMd neurons in broad-spiking (putative pyramidal) and narrow-spiking (putative interneurons) based on the trough-to-peak of their spike waveform. These two types of cell classes differed in their pattern of activity during both planning and execution of movement in a delayed reach task. Putative interneurons were more strongly modulated across conditions than pyramidal neurons, consistently with their larger dynamic range (Connors and Gutnick 1990), and were more likely to show increased firing rate during movement planning and complex modulation during various conditions. In contrast, putative pyramidal neurons showed more symmetric firing rate changes and the conditions causing suppression were almost as common as those producing excitation. In another study, Song and colleagues (Song and McPeek 2010) recorded PMd neurons during a reaction-time visual search task where monkeys reached to an odd-coloured target presented with distractors. They found that the distribution of extracellular spike waveforms duration (Figure 8A, B) was bimodal and allowed them to identify two distinct populations: narrow spiking neurons, ranging

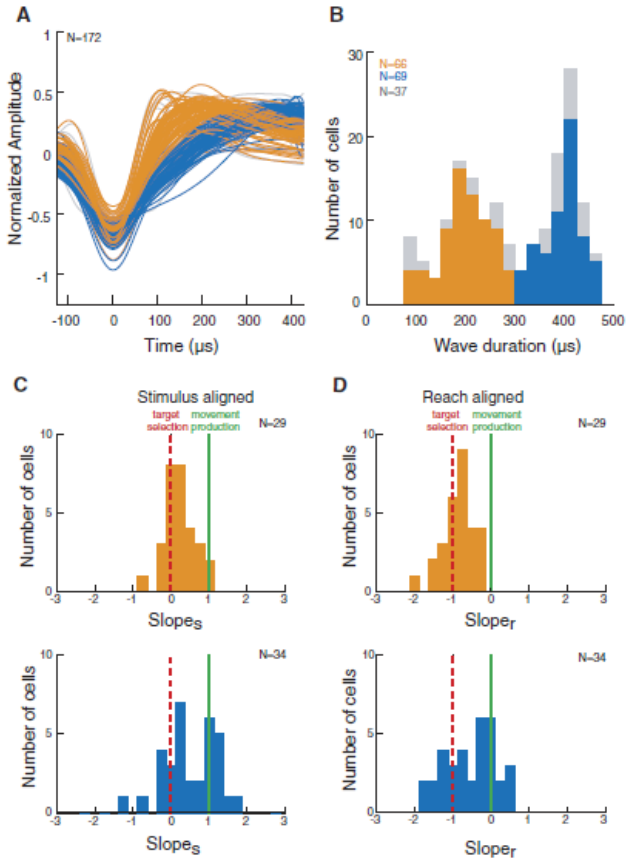

Figure 8. Extracellular Spike widths analysis. A: Normalized amplitude of all analysed neurons aligned relative to their troughs B: distribution of wave durations in narrow neurons (Orange) and broad neurons (blue) and non-task related neurons (gray)
C: Histograms of Slope$_s$=slope obtained from the stimulus-onset alignment Slope$_r$ = reach-onset alignment.
Top part for narrow-spiking neurons, bottom part for broad spiking neurons.
Modified by Song et al 2010

from 100 to 300 µs, and broadly spiking neurons, ranging from 301 to 500 µs (Figure 8B). In the same study, the authors showed that narrow-spiking neurons became active near the target selection (red dash line in Figure 8 C, D), whereas broad-spiking neurons activation was more shifted toward movement production (green line in Figure 8 C, D). Moreover, narrow-spiking neurons showed higher firing rates and earlier target selectivity as compared with broad-spiking neurons, which showed more mixed features. Previous evidence suggested that inhibitory interneurons have narrower action potentials than excitatory pyramidal cells (Connors and Gutnick 1990; Gold et al. 2006; González-Burgos et al. 2005; Henze et al. 2000; McCormick et al. 1985). On these bases, narrow and broad spiking neurons can be both involved in facilitatory target selection processes and inhibition of distractor stimuli, whereas movement execution involves essentially the output of broad spiking, putative pyramidal, PMd cells.

Other evidence indicates that neurons in monkey Frontal eye fields (FEF) (Cohen et al. 2009) recorded during memory-guided saccade tasks could be subdivided into three types of response patterns by measuring the spike width: visual, motor and visuomotor neurons. Motor neurons had the largest spike width, and visual neurons have larger spike width relative to visuomotor neurons that, in turn, showed the thinnest spikes. Different studies in FEF using the peak to trough found that broad- and narrow-spiking cells in

macaque differ during visual stimulation and attentional processes: narrow spiking cells have higher stimulus-induced firing rate and are more strongly affected by attention level with respect to broad-spiking cells (Thiele et al. 2016). Similar findings have been reported in many other studies on primate prefrontal cortex (PFC) neurons, which contributed to establish a distinction between the functional properties of narrow (putative interneurons) and broad (putative pyramidal) spiking neurons (Krimer et al. 2005; Mitchell et al. 2007; Diester and Nieder 2008; Shin and Sommer 2012; Johnston, et al 2009). The same distinction appears to be phylogenetically robust, as similar findings have been also reported in rats (Barthó et al. 2004).

Studies in medial superior temporal area (MSTd) and visual posterior sylvian fissure (VPS) in *Macaca Mulatta* (Zhang et al. 2018) clustered neurons in broad and narrow spiking cells using two parameters: the firing activity (pre stimulus and post stimulus) and the spike duration (Trought-to-peak). Narrow spiking neurons (considered as putative interneurons) responded to visual or vestibular signals with earlier peak time, higher firing rates and greater variability than broadly spiking neurons. It is clear, however, that the trough to peak seems to be the best candidate for characterizing this two cell groups. Physiologically, the extracellular spike waveform encompasses the repolarization phase of the membrane potential, and the difference between the spike duration in the interneurons and pyramidal cells are deemed to be due to different levels of expression of Na+ and K+ channels: fast spiking properties reflect the presence of Kv3 and Kv1, which allow fast repolarization (Härtig et al. 1999; Y Kawaguchi and Kubota 1997). On these basis, a further link between spike shape and discharge pattern criteria is that fast spiking neurons would correspond to narrow spiking (putative interneurons), whereas regular spiking neurons would correspond to broad spiking (putative pyramidal neurons).

3.2.3 Putative Interneurons and pyramidal cells

Pyramidal cells are estimated to form 70-80% of primates' neocortical neurons, being the remaining 20-30% constituted by interneurons (DeFelipe and Fariñas 1992; Markram et al. 2004; Elston et al. 2011). The former are deemed to exert their effect more globally, whereas the latter contribute to local processing. The proportion of the two types of cells may vary considerably between studies, with putative interneurons being estimated from 10-20% (Wilson et al 1994) to 20-30% (Barry W Connors and Gutnick 1990) or more

(Zhang et al. 2018). The possibility to distinguishing interneurons from pyramidal neurons based on extracellularly recorded spike features has been recently challenged, at least in the monkey frontal cortex, by studies on pyramidal tract neurons (PTNs) identified with antidromic stimulation in awake macaques' primary motor (M1) and ventral premotor (F5) cortex (Kraskov et al. 2009; Vigneswaran et al. 2011; 2013).

In these studies, the distribution of spike durations among PTNs was highly variable, including some PTNs with "thin" spikes that would otherwise be misattributed to putative inhibitory interneurons. The most intriguing and relevant finding is that spike width is negatively correlated with axon conduction velocity (i.e. antodromic latency), which means that the biggest pyramidal cells (with bigger and hence faster axons) are those that can be more frequently misclassified as interneurons. Furthermore, in the primate neocortical microcircuits, different studies have also supported the view that some interneurons have relatively broad spikes, hence showing that functional subdivisions into neuronal classes may not be so robust even when putative interneurons are concerned (Krimer et al. 2005; Torres-Gomez et al. 2020). Nonetheless, detailed descriptions of the possible relationship between functionally-classified neuronal classes and their properties in specific visuomotor tasks across and within cortical areas are lacking, and would strongly contribute to shape new hypothesis to bridge the gap between system-level and local processes in the organization and recognition of actions of self and others.

4. Aims of the study

The general aim of the present study consists in linking system-level investigation of neuronal properties in the main nodes of the AON with local circuitries and the possible differential role of functionally-defined neuronal classes in the processing of target objects and the actions of self and others. To achieve this goal, we extracellularly recorded neuronal activity from monkey's area AIP, F5 and F6 in the AON using the same execution (EXE) and observation (OBS) tasks. By applying a fully automated sorting algorithm (Chung et al. 2017), we extracted single neuron activity with the same restrictive criteria from all areas and:

1) compared single neuron and population codes in the three areas, regardless of the cell types, to obtain a functional fingerprint of areal specificities in planning, execution and observation of actions (system level);
2) identified distinct functional classes of cells, regardless of the area of origin, and studied their main functional specificities in the execution and observation tasks;
3) investigated possible local functional specificities in terms of cell classes in different areas and their contribution to areal functional specificities (local circuitries).

5. Materials and methods

Experiments were performed on three purpose-bred, socially housed adult macaques, Mk1 (*M. nemestrina,* male 9 kg), Mk2 (*M. mulatta,* male 7 Kg) and Mk3 (*M. mulatta,* Female 4 Kg). Neuronal activity in each area was recorded from two different monkeys (see Figure 9a). Before recordings, the monkeys were habituated to sit in a primate chair and to interact with the experimenters. Then, they were trained to perform an execution (EXE) and an observation (OBS) task (Bonini et al. 2014a), described below. When the training was completed, a head fixation system and different types of probes were implanted (during distinct surgeries) as previously described elsewhere (Bonini et al. 2014a; Bruni et al. 2015; Barz et al. 2017). All surgical procedures were carried out under general anaesthesia (ketamine hydrochloride, 5 mg/kg intramuscularly [i.m.] and medetomidine hydrochloride, 0.1 mg/kg, i.m), followed by postsurgical pain medications. The experimental protocols complied with the European law on the humane care and use of laboratory animals (Directive 2010/63/EU), were approved by the Veterinarian Animal Care and Use Committee of the University of Parma (Prot. 78/12, 17/07/2012 and Prot. 91/OPBA/2015) and authorized by the Italian Ministry of Health (D.M. 294/2012-C, 11/12/2012 and 48/2016-PR, 20/01/2016).

5.1 Apparatus and behavioural paradigm

The apparatus for the visuomotor (EXE) and observation (OBS) tasks (Figure 9b) was described in details in a previous work (Bonini et al. 2014a). During EXE, the monkey was seated on a primate chair in front of a box, divided horizontally into 2 sectors by a half-mirror where a spot of light (fixation point) was projected in the exact position of the centre of mass of the not-yet-visible target object. The objects (a ring, a small cone, and a big cone) were presented randomly, one at a time, at a reaching distance from the monkey's hand starting position. The objects afforded three different grip types: hook grip (ring), precision grip (small cone), whole-hand prehension (big cone). The task included two basic conditions, Go and No-Go, and each trial was preceded by a variable (from 1 to 1.5 s) inter-trial period.

Go condition. The fixation point was presented, and the monkey was required to start fixating it within 1.2 s. Fixation onset resulted in the presentation of a cue sound (high

tone, 1200 Hz), which instructed the monkey to grasp the subsequently presented object (Go cue). After 0.8 s one of the objects became visible. Then, after a variable time lag (0.8–1.2 s), the sound ceased (Go signal), and the monkey had to reach, grasp, and pull (for 0.8 s) the object within 1.2 s to get a fixed amount of juice reward (automatically delivered).

No-Go condition. The sequence of task events in this condition was the same as in the Go condition but a different cue sound (low tone, 300 Hz) instructed the monkey to remain still and fixate the object for 1.2 s after the end of the sound, in order to receive the reward.

The same sequence of events described for EXE also applied to OBS, in which an experimenter performed the task in the monkey extrapersonal space, seen by the monkey from a 90° visual perspective (Bonini et al. 2014b).

Contact sensitive devices (Crist Instruments) were used to detect when the monkey (grounded) touched the metal surface of the starting position or one of the target objects. To signal the onset and tonic phase of object pulling, an additional device was connected to the switch located behind each object. Custom-made LabView-based software was used to monitor the monkey's performance and to control the presentation of auditory and visual cues (see for details Bonini et al., 2014a). Eye position was monitored at 50 Hz with a camera-based eye tracking system and the monkey was required to maintain its gaze on the fixation point with a tolerance radius of 5° throughout the task. If the monkey broke fixation, made an incorrect movement, or did not respect the task temporal constraints, no reward was delivered and the wrong trials was put back in the randomized list to be subsequently repeated. We collected at least 10 correctly performed trials for each condition.

5.2 Recording Techniques

Neuronal recordings were performed by means of multielectrode linear silicon probes in different single-shaft (Bonini et al. 2014a; Ferroni et al. 2017) or 3D (Barz et al. 2017) configurations, implanted chronically in AIP (Lanzilotto et al. 2019) and F6 (Lanzilotto et al. 2016) and acutely in F5 (Bonini et al. 2014a), based on MRI reconstruction of the target brain regions. Analog signal from all the recording electrodes was simultaneously amplified and sampled either at 30 kHz with an Open Ephys system (http://open-ephys.org/) or at 40 kHz with an Omniplex system (Plexon).

All formal signal analyses were performed offline. Spike sorting was performed with fully automated software, Mountainsort (Chung et al. 2017), using -3.0 SDs of the signal-to-noise ratio of each channel as the threshold for detecting units. To exclude that possible artifacts were counted as spikes, we automatically inspected all waveforms of all isolated units and retained, for each unit, only those waveforms that did not exceed ±3 SD from the average waveform in all data points (approximately 10% of the waveforms in each unit were removed with this procedure). To identify single- vs multi-units, we used the noise overlap, a parameter that can vary between 0 and 1, with units with a value below 0.1 being considered as single units. Single unit isolation was further verified using standard criteria (ISI distribution, refractory period > 1 ms, and absence of cross-correlated firing with time-lag of ≈ 0 relative to other isolated units, to avoid oversampling).

To obtain the average waveform for each individual unit we randomly selected from the filtered signal 1000 of its spikes in a window of 2.5 ms centred on the absolute minimum. Each waveform was spline interpolated in order to achieve 1000 points in the 2.5 ms window, regardless of the original sampling rate, and realigned to the absolute minimum. This procedure produced the average waveform for all units. Then, we obtained the final data set by excluding all units with 1) less than 1000 spikes; 2) very noisy waveforms (multi-peak, e.g. multiple local maxima between the main trough and the subsequent peak); 3) a main trough amplitude smaller than the subsequent peak or a peak before the trough greater than 20% the trough depth amplitude, since they likely belong to axon fibres (Gold et al. 2006; Robbins et al. 2013). The final data set included 355 single neurons fulfilling all these criteria.

5.3 Clustering of single-neuron waveforms

For clustering neurons based on their waveform we considered the two most widely established waveform parameters, namely, trough-to-peak duration (Vigneswaran, Kraskov, and Lemon 2011; Kaufman et al. 2010) and repolarization time (Ardid et al. 2015). The trough-to-peak duration is the interval between the global minimum of the curve and the following local maximum. The repolarization time is the interval between the late positive peak and the subsequent inflection point (where the second derivative equals zero).

To identify clusters of waveforms based on these two parameters, we followed a recently described procedure (Trainito et al. 2019) consisting in calculating the optimal number of clusters by fitting the two-dimensional data as a Gaussian mixture distribution and taking as the number of clusters the one that minimize the Bayesian Information Criterion (BIC, Figure 12a). Since the selected parameters (trough-to-peak duration and repolarization time) were clearly correlated (correlation coefficient $R=0.52$, $p=7\cdot10^{-26}$), we imposed a diagonal covariance matrix when fitting the data and obtained three clusters including a variable number of neurons. Previous studies adopted an additional outlier removal procedure leading to the exclusion of approximately 11% of the neurons (Trainito et al. 2019); this procedure would have a similar impact on our dataset, with 12.7% of the neurons excluded, but more than 80% of them belonging to cluster 3, which includes the greatest number of neurons. Thus, we decided not to add further exclusion criteria to those described above.

5.4 Population analyses

For each neuron, we first computed its baseline firing rate (corresponding to the 500 ms time interval preceding Cue-Sound presentation) for EXE and OBS (objects and trials averaged), separately. We then computed the net normalized activity of each neuron. First, we subtracted its baseline activity in a given condition from the firing rate of each bin; then, we soft-normalized the resulting net activity vector by dividing each data point by the absolute maximum across all conditions + 5 spk/s (this latter constant factor reduces the overall net normalize activity of neurons with very low firing rate). The resulting net normalized activities (ranging theoretically between -1 and 1) were used to produce the heat-maps, to show individual neurons firing rate in a comparable form during EXE and OBS task unfolding periods.

Neurons were subdivided in facilitated or suppressed depending on the sign of the average modulation they showed during the movement period (action execution or observation in the time interval ranging from -300 ms before +900 ms after the Go signal). To test if the modulation of facilitated (red lines in Figure 10 and Figure 15) and suppressed (blue lines in Figure 10 and Figure 15) neurons was statistically significant, we compared their baseline activity with each bin of the movement period (sliding t-test, window=200 ms, step=20 ms, $p<0.05$, uncorrected) in the -300/+900 ms interval around Go signal during the whole movement period of EXE and OBS. We considered

significantly facilitated or suppressed all those neurons with at least 5 consecutive significant bins. Neurons that did not meet this criterion were classified as non-significantly modulated. Peak times of facilitated neurons were calculated in 0.1-0.5 time interval after object presentation and in 0-0.6 time interval after Go-signal.

5.5 Decoding analyses

To compare how information about task parameters was represented in different areas we employed the Neural Decoding Toolbox (Meyers 2013) already used in our previous studies (Lanzilotto et al. 2019; Livi, Lanzilotto, et al. 2019; Lanzilotto et al. 2020). Specifically, we assessed the decoding accuracy of a Poisson naïve Bayes classifier trained and tested to classify different variable, that is, Go/No-Go or type of object (Figure 10, Figure 11).

Regardless of the decoded variable, for each neuron data were first converted from raster format into binned format. Specifically, we created binned data that contained the average firing rate in 200 ms bins sampled at 20 ms intervals for each trial (data-point). We obtained a population of binned data characterized by a number of data points corresponding to the number of trials per conditions (i.e. 30 x 2 = 60 data-points for Go/No-Go decoding; 10 x 3 = 30 data-points for object decoding) in an N-dimensional space (where N is the total number of neurons considered for each analysis). Next, we randomly grouped all the available data points into a number of splits corresponding to the number of data points per condition, with each split containing a "pseudo-population", that is, a population of neurons that could be partially recorded separately but treated as if they were recorded simultaneously. Before sending the data to the classifier, we pre-selected those features (neurons) that showed a difference between conditions with $p<0.5$. Subsequently, the classifier was trained using all but one of the splits of the data and then tested on the remaining one. This procedure was repeated as many times as the number of splits (i.e., 30 in the case of Go/No-Go decoding, 10 in the case of object decoding), leaving out a different test split each time.

As a measure for the performance of the classification we used the mutual information (MI, see Quiroga and Panzeri 2009), defined as the reduction of uncertainty (or gained information) about the current condition obtained by knowing the neuronal response. The greater the amount of information carried by the population, the smaller the uncertainty on the current condition. When the probability of presenting each of *K*

different conditions is equal, MI can reach a theoretical maximum of log_2K (i.e. 1 for Go/No-Go decoding and 1.585 for object decoding); we used this values to normalize MI corresponding curves in Figure 10 and 11. Because, on average, the higher the number of neurons used in the decoding the higher the performance of the classifier, we performed a number-matching procedure to make the results of different areas comparable. To this purpose, we performed the decoding analysis on randomly selected sets of 65 neurons from each area (with replacement), corresponding to 3/4 of the neurons in AIP (n= 86), which is the area with the lowest number of neurons. We repeated this procedure 50 times (each of them averaged across 10 runs with different data in the training and test splits from the same set of neurons, to increase the robustness of the result, and smoothed with a 40 ms Gaussian kernel). We finally computed the mean and the standard deviation (shading in Figure 10) of the resulting distribution.

To assess statistically when each area starts to convey a given type of information (i.e. Go/No-go or object/grip type), we calculated for each iteration of the procedure described above the time point where the mutual information exceeds 1/3 of its maximum theoretical value. This was repeated with all iterations and the standard deviation of the resulting time point distribution (multiplied by $65/N_{area}$ in order to consider the different subsample size with respect to the reference population) was taken as standard error. We finally compared the mean onset among areas by performing multiple two-tailed two-sample z-test (p values uncorrected).

5.6 Index of Mutual Modulation Depth

To the purpose of comparing the dynamic (positive or negative) modulation of single neuron discharge in corresponding time bins of EXE and OBS, we conceived an index quantifying the mutual modulation depth (MMD). For each neuron, in the interval -500/700 ms relative to the movement onset, we calculated the net soft-normalized activity (as described above) for EXE and OBS, separately, smoothed with 200 ms bins advanced in steps of 20 ms. Then, the MMD was computed for each neuron bin-by-bin as the product of EXE and OBS activity values. Neurons showing a similar discharge profile in both EXE and OBS (regardless of whether it was jointly facilitated or suppressed) showed positive MMD values: the closer to 1 (theoretical value) the greater the (positive or negative) discharge modulation (Figure 18a, b). In contrast, neurons showing large but opposite modulation (facilitated/suppressed or vice versa), showed negative MMD

values: the closer to -1 (theoretical value) the greater the EXE and OBS opposite modulation (Figure 18c, d). If in one condition the neuron does not modulate its discharge, the index become close to 0 regardless of the behaviour of the neuron in the other condition because of multiplication by zero (Figure 18e, f).

To assess the overall significance of MMD in a given subpopulation of neurons, we compared the average MMD of every bin with a chance value calculated in the first 5 bins (300 ms of activity) of each plot. We applied this procedure on the entire data set by repeatedly shuffling (10^4 iterations) the 355x5 (neurons x bins) matrix, taking at each iteration the average of N random MMD values, where N correspond to the number of neurons in each subpopulation of cluster x area. We thus obtained nine null distributions of MMD values, and the 99^{th} percentile of each of them was adopted as a criterion ($p=0.01$) to set a significance threshold for the corresponding subpopulation (Figure 18g). We required at least 5 consecutive bins to be significant to plot the result (black line on top of each plot of Figure 18g).

6. Results

We isolated 355 single neurons from chronic multielectrode recordings carried out in three monkeys and from three different cortical areas (Figure 9a): AIP (n=86), F5 (n=106) and F6 (n=163). All units with atypical waveform features relative to a pre-defined set of criteria (see Methods) and/or with less than 1000 spikes in the whole recording session were excluded from the data set (n=81, 18.6%). During the recordings, monkeys performed an execution task (EXE, Figure 9b) and observed the same task performed by an experimenter (OBS, Figure 9b). The temporal structure of task events was the same in both tasks (Figure 9c).

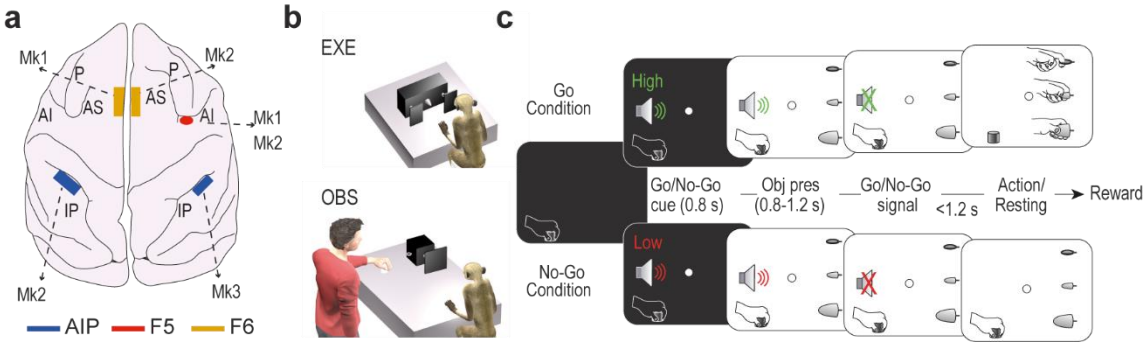

Figure 9. Recorded regions and behavioral task
(a) Schematic reconstruction of the recorded regions in the three animals reported on Mk1's brain.
(b) Behavioral setting for the execution (EXE) and observation (OBS) task.
(c) Temporal sequence of events of the Go/No-Go visuomotor task. The monkey starts with its hand in a fixed position. The onset of central fixation in the position where the object is presented triggers a Go/No-Go auditory cue (high/low frequency sound, respectively). Following a variable delay after object presentation, the end of the sound (Go/No-Go signal) instruct the monkey to reach and grasp the visually presented object or to remain still until the end of the trial to obtain the reward.

6.1 Functional fingerprint of parietal and frontal areas during task execution and observation

To investigate the time course and functional specificities of neuronal processing during the tasks in the three areas, we first classified each neuron as facilitated (red), suppressed (blue) or non-significant (white) depending on its modulation during action execution (Figure 10a) and observation (Figure 10b) relative to baseline (see Methods).

During EXE (Figure 10a), in AIP and F5 we found a similar fraction of facilitated and suppressed neurons (AIP vs F5: $\chi^2 = 0.04$, p=0.8354), with an overall prevalence of

facilitated ones, which both differed from F6 where, instead, cells with suppressed response prevailed (F6 vs AIP: χ^2=8.62, p=0.0033; F6 vs F5: χ^2=12.22, p=0.0005). Facilitated neurons exhibited a clearly measurable peak of activity already in relation to the visual presentation of the object, first in AIP (+220 ms) and F5 (+240 ms) and later on in F6 (+300 ms, Kruskal-Wallis test, F6 vs AIP χ^2=8.70 p=0.013; F6 vs F5 χ^2=5.65 p=0.059, see Methods). In contrast, the peak of population activity relative to the Go-signal showed the opposite trend, occurring earlier in F6 (+160 ms) than in both F5 (+400 ms, χ^2=8.60 p=0.014) and AIP (+420ms, χ^2=6.57 p=0.037), which in turn did not significantly differ from each other (χ^2=0.026 p=0.987).

To better investigate the time course of different signals across the studied areas, we performed a neural decoding analysis (Meyers 2013) by training and testing a Poisson naïve Bayes classifier to discriminate between Go and No-Go conditions based on population activity of each area (see Methods). The results (Figure 10c) show that the mutual information distinguishing Go and No-Go trials became significant very early in area F6 (-280 ms from object presentation) relative to F5 (+100 ms, z-test on subsampling repetitions Z=2.60 p=0.0092) and AIP (+440 ms, Z=6.59 p=$4.3\cdot10^{-11}$), with F5 significantly preceding AIP (Z=2.46 p=0.0138). Conversely, mutual information about the type of target object rises first in AIP (since 180 ms after object presentation), shortly after in F5 (200ms) and finally in F6, significantly later (240ms) with respect to AIP (Z=2.25 p=0.024) but not to F5 (Z=1.68 p=0.092). Object-selective signal was not only earlier, but also stronger in AIP and F5 relative to F6, where the mutual information about object type remained smaller than in the other two areas for the entire duration of the trial (Fig 10c, lower part). Interestingly, a stronger and earlier contribution of AIP in signaling the type of object is also evident by analysing neuronal population response during No-Go trials (Figure 11a and b), supporting a predominantly visual nature of AIP object-related signal relative to F5 and F6.

Altogether, these findings highlight a greater similarity of the lateral convexity areas AIP and F5 relative to F6, with the AIP-F5 circuit playing a major role in the processing of graspable objects and reaching-grasping actions by linking visual features of the target, encoded in AIP, with specific motor plans for grasping it, primarily represented in F5 (Fogassi et al. 2001; Schaffelhofer and Scherberger 2016). In contrast, area F6 strongly differs in terms of timing and strength of its object- and action-related tuning, showing earlier and predominantly suppressed activity signalling whether a forthcoming action will be performed or withheld.

During OBS (Figure 10b), the modulation depth of both facilitated and suppressed neurons response was overall smaller than in EXE, in all the investigated areas. The number of facilitated and suppressed neurons was perfectly balanced in AIP, similarly to F5 (χ^2=0.66, p=0.4175) where facilitated neurons where slightly prevalent; in contrast, in F6, suppressed neurons clearly prevailed, especially relative to F5 (F6 vs F5 χ^2=10.31, p=0.0013; F6 vs AIP χ^2=4.27, p=0.0388). The fraction of non-significant cells slightly increased in OBS relative to EXE in all three areas; nonetheless, area F5 still exhibited a clear-cut, event-related modulation during agent's reaching-grasping action due to the prevalence of facilitated neurons, which exhibited a measurable peak of activity in correspondence with the observation of object pulling onset. Instead, areas AIP and F6, despite hosting single neurons with phasic facilitated activity related to reaching-grasping observation (see heat map in Figure 10b), did not show any transient modulation of their population response.

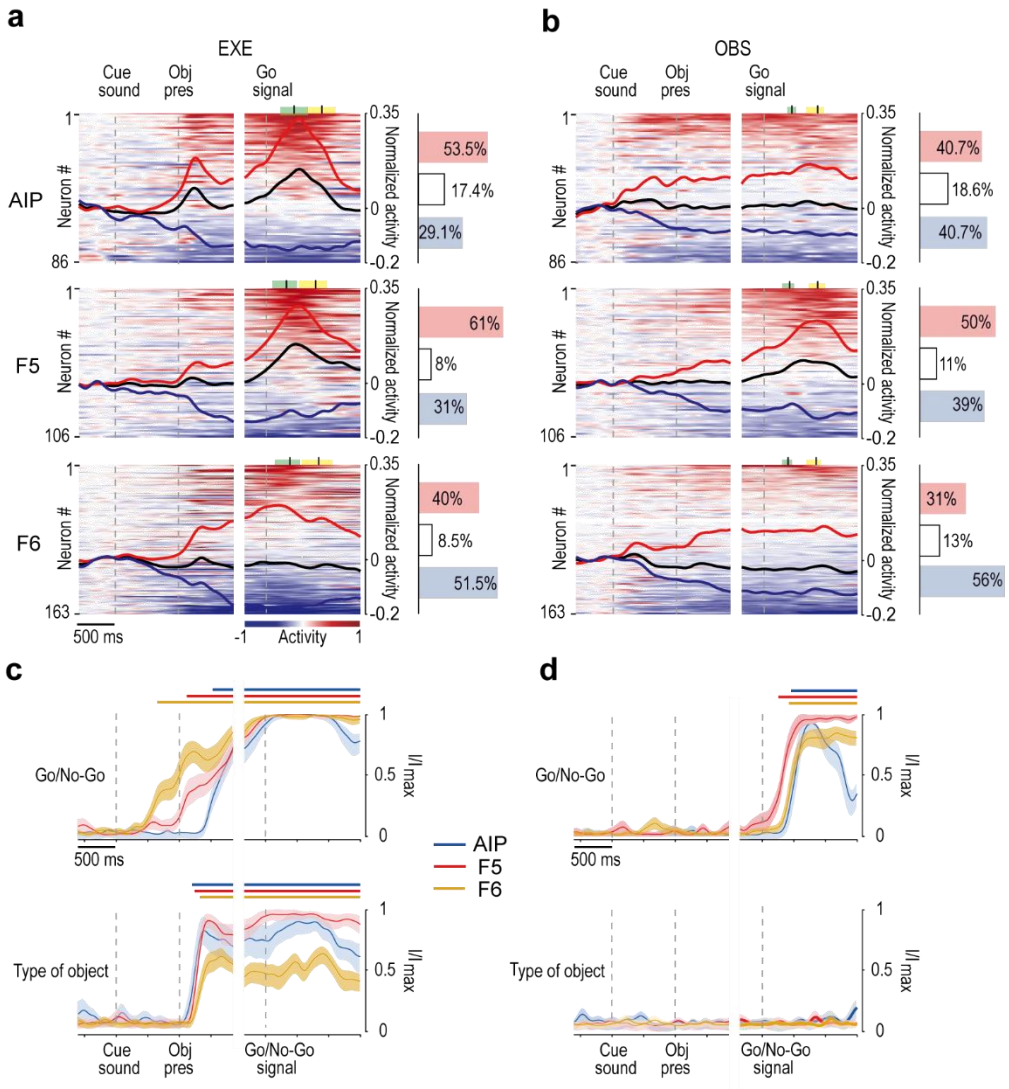

Figure 10. **Functional properties of AIP, F5 and F6 in EXE and OBS.**
(a) Heat maps of all the recorded neurons in each area during EXE. Each line represents one cell, and cells are ordered (from top to bottom) based on the magnitude of their activity with respect to baseline (red = facilitated, blue = suppressed) in the interval between 300 ms before until 900 ms after Go-signal. Black lines represent the averaged response of each population as a whole. The histograms on the right indicate the percentage of facilitated (red), suppressed (blue) and non-significant (white) neurons in each area (see Materials and Methods).
(b) Heat maps and population response of all the recorded neurons in each area during OBS. Data have been normalized together with EXE to facilitate comparisons. All conventions as in (a). Note that the neurons have been ordered independently from panel (a). Heat maps of all the neurons shown in A recorded during OBS. Conventions as in A.
(c) Mutual information on Go/No-Go trials (top) and type of object (bottom) during EXE decoded from neuronal population activity of each area along the task unfolding period. Continuous colored bars on top of each plot indicate the period in which the decoding accuracy is significantly higher than chance (z-test on real versus shuffled data, see Materials and Methods).
(d) Mutual information about Go/No-Go (top) and type of object (bottom) during OBS. Conventions as in (b).

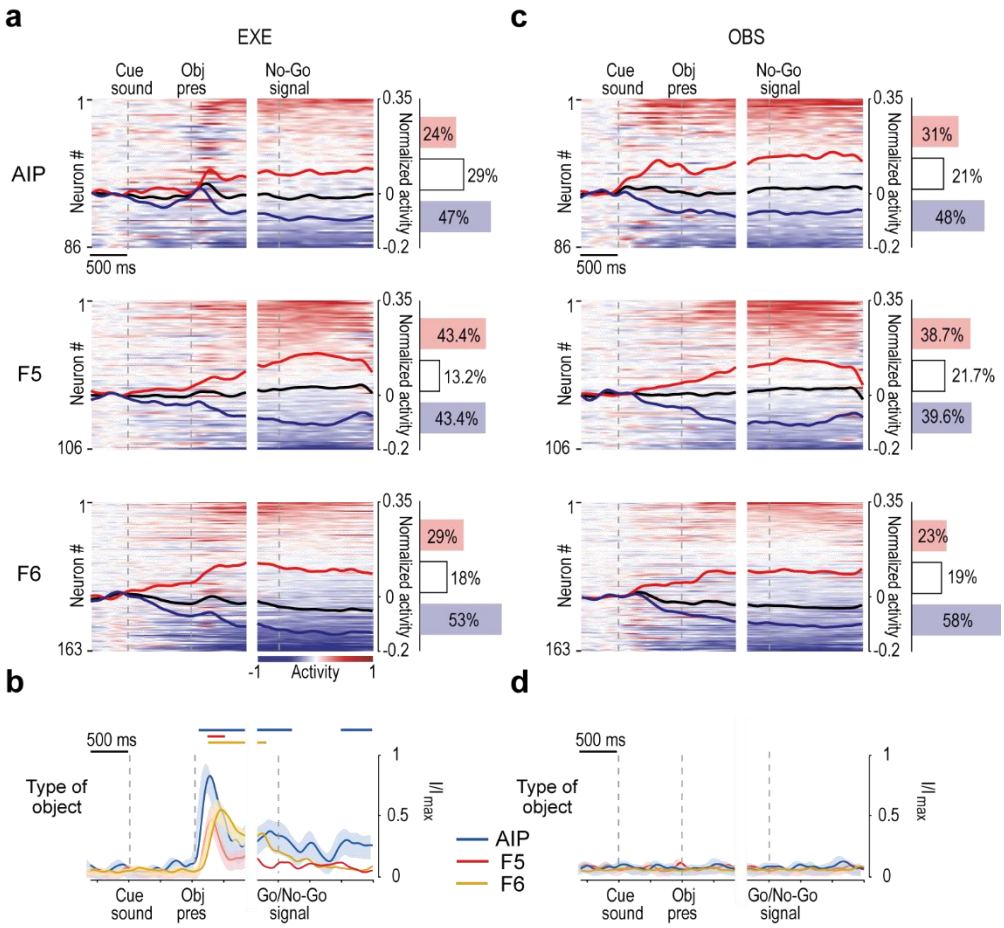

Figure 11. **Functional properties of AIP, F5 and F6 neurons during No-Go trials of EXE and OBS.**
(a) Heat maps of all the recorded neurons in each area during No-Go trials of EXE. Each line represents one cell, and cells are ordered (from top to bottom) based on the magnitude of their

activity with respect to baseline (red = facilitated, blue = suppressed) in the interval between 300 ms before until 900 ms after the No-Go signal. Black lines represent the averaged response of each population as a whole. The histograms on the right indicate the percentage of facilitated, suppressed and non-significant neurons in each area (see Materials and Methods).

(b) Mutual information on type of object in EXE No-Go trials decoded from neuronal population activity of each area along the task unfolding period. Continuous colored bars on top of each plot indicate the period in which the decoding accuracy is significantly higher than chance (z-test on real versus shuffled data, see Materials and Methods).

(c) Heat maps and population response of all the recorded neurons in each area during OBS. All conventions as in (a). Note that the neurons have been ordered independently from panel (a).

(d) Mutual information on type of object (bottom) of OBS. Conventions as in (b).

By applying the neural decoding approach to OBS (Figure 10d), the classifier could detect significant mutual information discriminating between Go and No-Go trials only during the movement epoch, essentially revealing a robust signal related to action observation in all three areas. However, as compared to EXE (Figure 10c), we found no additional object or observed grip-type specificity during OBS. Interestingly, significant mutual information about Go/No-Go raises earlier in F5 (+200 ms relative to the Go/No-Go signal) than in F6 (+360 ms, $Z=2.90$ $p=0.0038$) and AIP (+400 ms, $Z=3.11$ $p=0.0019$). Because neurons in different areas were not recorded simultaneously, hence being potentially subject to variation in the reaction time of the actor, we also repeated this analysis by aligning the activity to reaching movement onset: the findings confirm the earlier activation of area F5 (-260 ms relative to movement onset) with respect to both AIP (-40 ms, $Z=3.55$ $p=3.8\cdot10^{-4}$) and F6 (0 ms, $Z=3.23$ $p=0.0012$). These data provide strong support to the idea that, in the action observation network, area F5 does not necessarily need to be triggered by visual information about other's action coming from the parietal cortex (Ferrari et al. 2009; Bonini 2017), but can also predictively represent upcoming actions of others (Maranesi et al. 2014) with inherently generative capacities (Umiltà et al. 2001; Bonini et al. 2014b; Caggiano et al. 2016).

6.2 Identification and functional properties of cell classes based on extracellular spike waveforms

Next, we wanted to investigate cell-class specificities of each of the areas described so far. To this purpose, we first measured two parameters of spikes waveforms for all the neurons isolated in the three investigated areas, namely, trough-to-peak duration and

repolarization time (Trainito et al. 2019). The trough-to-peak defines the spike amplitude in terms of the interval between the global minimum of the spike shape and the following local maximum, whereas the repolarization time is the interval between the local maximum following the global minimum and the subsequent inflection point of the curve (Figure 12a).

To identity two-dimensional clusters with the available parameters and waveforms, we adopted an unsupervised clustering procedure (Gaussian mixture model, see Methods). A Bayesian information criterion (BIC) indicated the optimal number of Gaussian components (i.e. three waveforms classes) in our data set (Figure 12a, inset). The overall representation of the clustering results revealed three neuronal classes ranging from narrow spiking (class 1) to broadly spiking (class 3) neurons, with a clear prevalence of broadly spiking neurons (Figure 12b), in line with previous studies (Kaufman et al. 2010; Kaufman et al. 2013; Hussar and Pasternak 2009; Mitchell et al. 2007).

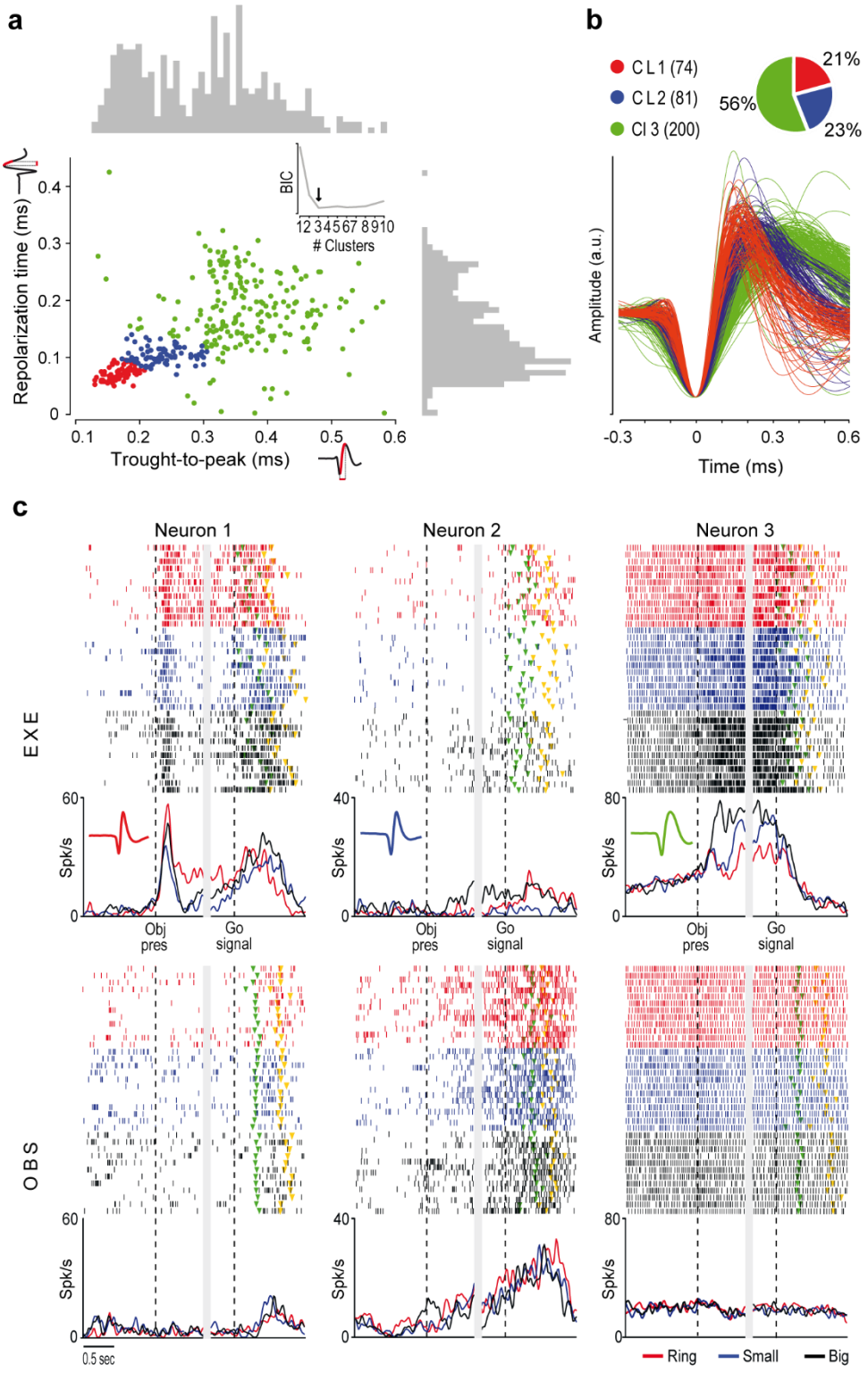

Figure 12. Clustering and properties of spike waveforms recorded from the three areas.
(a) Projection of each spike waveforms in the 2D space formed by trough-to-peak and repolarization time. Color codes identify the clusters (cell classes) resulting from the Gaussian mixture model applied with the number (n=3) of components indicated by the Bayesian information criterion (BIC) shown in the inset.
(b) Number of neurons in each cell class (in color code) in the whole data set, and individual average spike waveforms belonging to each class.

(C) Example neurons recorded in AIP, F5 and F6 (from Neuron 1 to 3), belonging to each of the three classes (spike waveform is shown in color code in the inset of each histogram, as in B). Activity is aligned (vertical dashed lines) on object presentation (Obj pres) and then (after the gap) on the Go signal, in both tasks. Each color refers to trials with one type of target object: a ring (red), a small cone (blue) and big cone (black).

Figure 12c shows representative examples of single neurons belonging to each of the three classes (individual neurons' waveform is shown in the inset; color code as in B). Neuron 1 is an AIP cell belonging to class 1: during EXE, this neuron discharged vigorously to the presentation of the object and, subsequently, while grasping it, but it also fired during experimenter's grasping in OBS. Neuron 2 was recorded from area F5 and belongs to class 2: it discharged during grasping of the ring and of the big cone in EXE and, even stronger, during experimenter's grasping in OBS, but with no selectivity for the target object in this task. Finally, Neuron 3 is an F6 cell belonging to class 3: it smoothly increased its firing rate following object presentation in EXE, reaching its peak prior to the go signal with remarkable object selectivity and showing no significant modulation of its discharge during OBS.

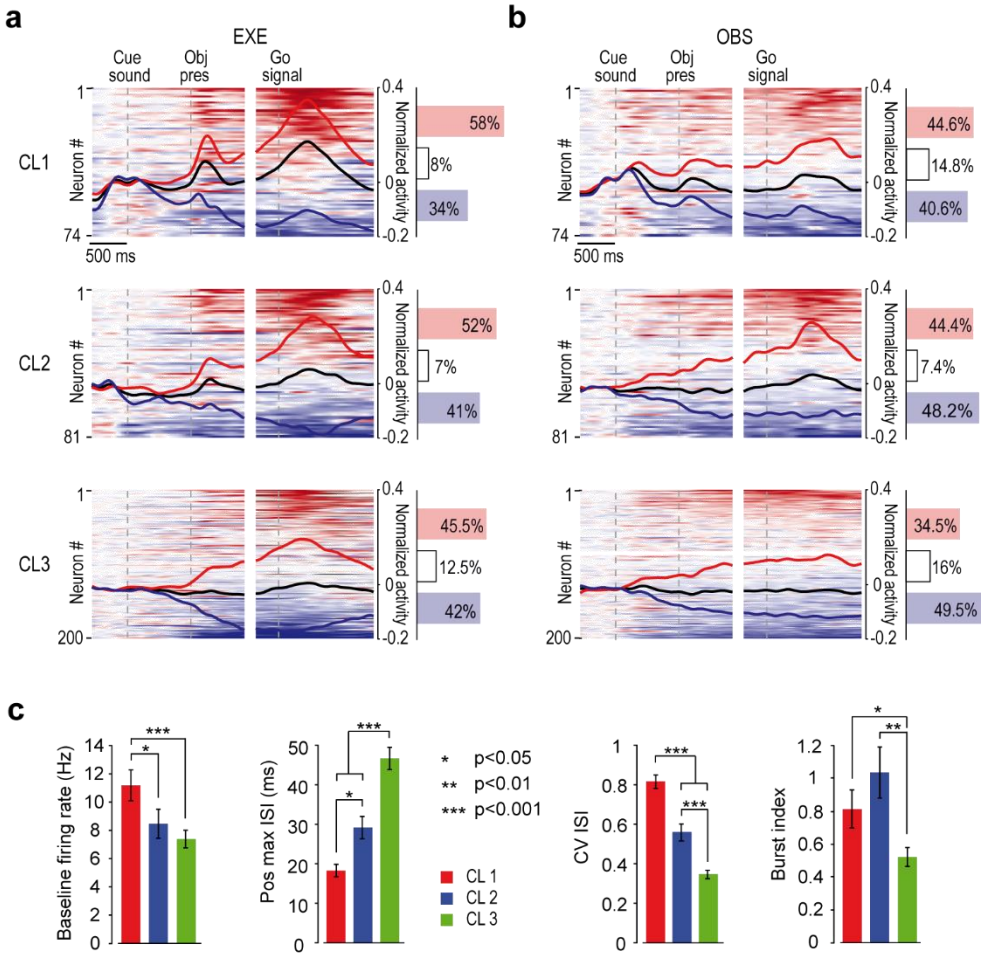

Figure 13. Tuning and firing properties of neurons in different cell classes.

(a) Heat maps and population response of all the recorded neurons in each cluster during EXE. All conventions as in Figure S1A (all χ^2 comparisons between pairs of clusters $p>0.11$).

(b) Heat maps and population response of all the recorded neurons in each cluster during OBS. All conventions as in Figure S1A (all χ^2 comparisons between pairs of clusters $p>0.12$).

(c) From left to right: average baseline firing rate of each cluster during EXE (Mann-Whitney test); average position of the maximum of the ISI distribution (Mann-Whitney test); coefficient of variation of the ISI distribution (one-way ANOVA $p<0.001$, Tukey-Kramer post-hoc); average Burst index, calculated as the ratio of ISI intervals < 5ms divided by all intervals < 100ms, normalized by the same ratio that would be expected by a Poisson process of equal mean rate (Mann-Whitney test). Error bars within each plot indicate standard errors.

By comparing the tuning and the firing properties of the cells in the three classes (regardless of the anatomical areas they were recorded from), we reported several distinctive features. Although we found a generally greater number of facilitated than suppressed neurons (especially in class 1), their relative proportion did not differ significantly across classes neither in EXE (Figure 13a) nor in OBS (Figure 13b); nonetheless, facilitated cells of class 1 and 2 showed stronger tuning to visually presented objects, executed and observed actions relative to cells of class 3 (Figure 14). Thus, neurons with narrower spikes appear to be more sharply tuned to visual and visuomotor information than broadly spiking neurons. In line with this latter observation, the firing statistics of the identified cell classes (Figure 13c) indicate that narrow spiking neurons exhibit greater baseline firing rate, shorter and more variable inter-spike interval (ISI), as well as a higher tendency to fire in burst relative to broadly spiking neurons, which in turn show slower and more regular firing pattern.

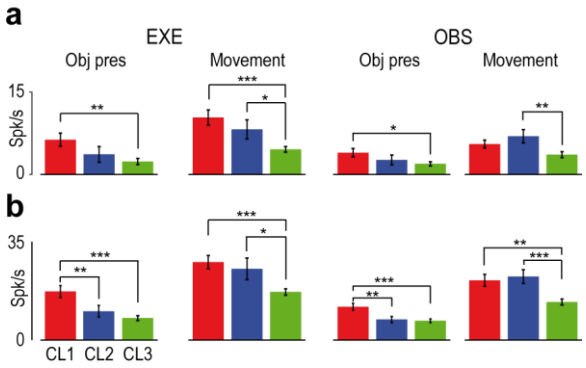

Figure 14. **Cell-class response properties during EXE and OBS.**

Cell-class response properties during EXE and OBS. (a) Average net firing rates of facilitated neurons of cell class 1 (red), 2 (blue) and 3 (green) during object presentation (0.1-0.3 relative to Object presentations) and movement epoch (-0.3 -0.9 relative to Go-signal) in EXE (left) and OBS (right) tasks. (b) Average peak of net firing rates of facilitated neurons of the three cell

classes during object presentation (0.1-0.3 relative to Object presentations) and movement epoch (-0.3 -0.9 relative to Go-signal) in EXE (left) and OBS (right). Conventions as in (a). * $p<0.05$; **$p<0.01$; ***$p<0.001$.

6.3 Functional specificities of cell classes in AIP, F5 and F6

Based on the findings so far presented, next we asked whether the identified cell classes differently contribute to the functional specificities of the three investigated areas. By comparing the overall distribution of neurons in the three classes (see Figure 12b) with that obtained in each area (Figure 15a), we found no significant deviation in AIP (χ^2 = 1.19, p=0.55), whereas F5 have a greater fraction of neurons in the first two classes and a smaller number in the third class (χ^2 = 18.27 p=0.0001), and F6 exhibit the opposite trend, with a greater fraction of neurons in the third class (χ^2 = 10.57 p=0.005).

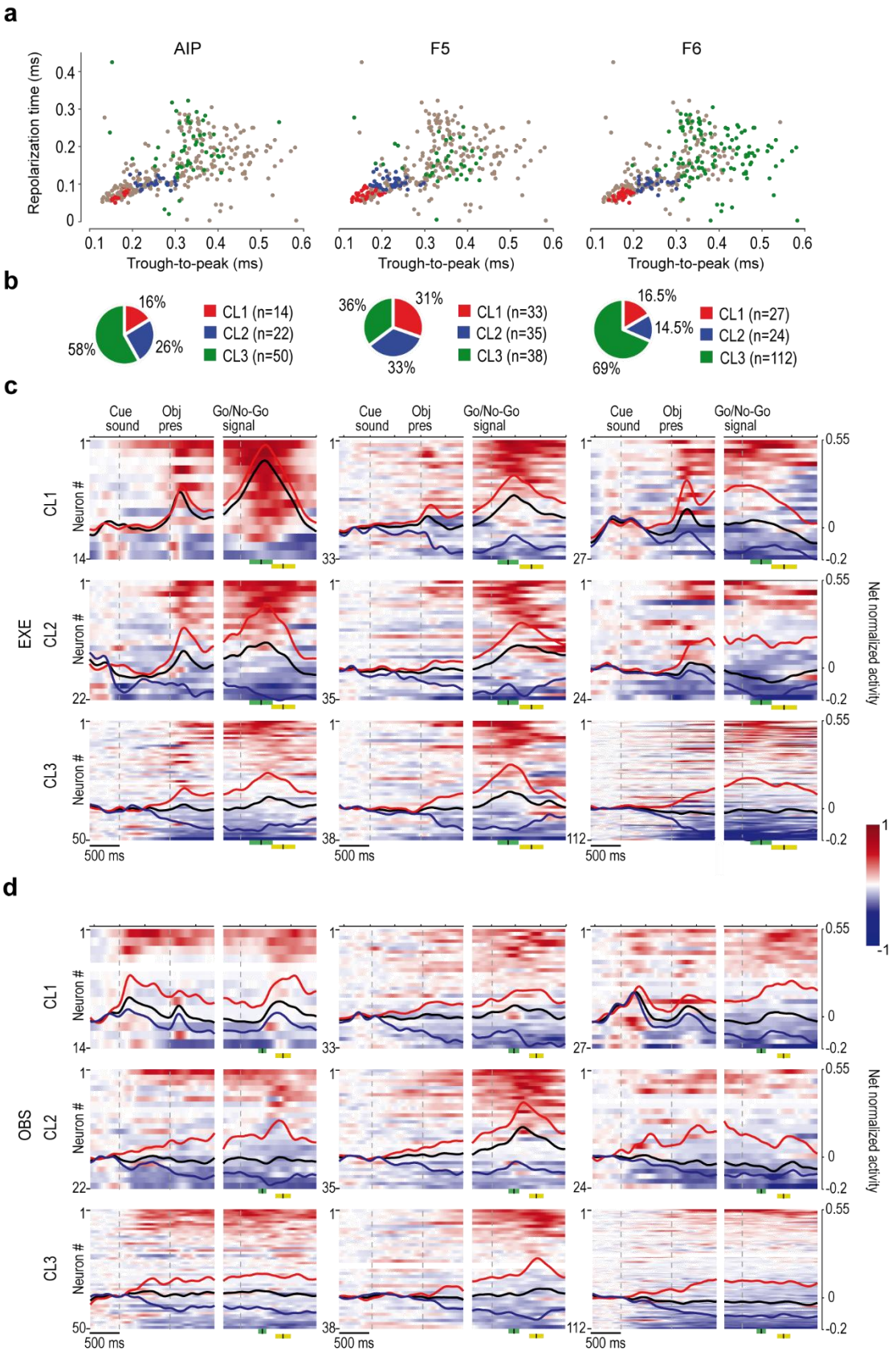
a
AIP
F5
F6
Repolarization time (ms)
Trough-to-peak (ms)
b
16%
58%
26%
CL1 (n=14)
CL2 (n=22)
CL3 (n=50)
36%
31%
33%
CL1 (n=33)
CL2 (n=35)
CL3 (n=38)
16.5%
14.5%
69%
CL1 (n=27)
CL2 (n=24)
CL3 (n=112)
c
Cue sound
Obj pres
Go/No-Go signal
EXE
CL1
CL2
CL3
Neuron #
500 ms
Net normalized activity
d
OBS
CL1
CL2
CL3
Neuron #
500 ms
Net normalized activity

Figure 15. **Functional properties of cell classes in AIP, F5 and F6 during EXE and OBS.**

(a) Projection of each spike waveforms in the 2D space formed by trough-to-peak and repolarization time. Color codes identify the cell class to which each neuron of a given area has been attributed; grey dots in each plot correspond to the neurons that do not belong to the corresponding area. Other conventions as in Fig 12a.
(b) Number of neurons of each cell class (in color code) in each area, expressed as a percentage of the total number of neurons recorded in each area.
(c) Heat maps and population response of all the recorded neurons recorded in each area during EXE, subdivided into the cell classes to which they belong. Conventions as in Fig 10a. Green and yellow marks represent average ± standard deviation of movement onset and pull, respectively.
(d) Heat maps and population response of all the neurons recorded in each area during OBS, subdivided into the cell classes to which they belong. Conventions as in Fig 10.

Next, we asked whether and how the uneven representation of neuronal classes in the three areas impacted in their overall output signal during EXE and OBS. To this purpose, we analysed the response of neurons (raw firing rate) in the different classes recorded from the three areas during EXE (Figure 15b) with a 3 x 3 x 3 repeated measures ANOVA (within factor: Epoch), with Cell class and Area as grouping factors, followed by Newman-Keuls post-hoc test where appropriate. The results (Figure 16) indicate that neurons of area F5, regardless of the cell class, showed the overall higher firing rate among the three areas ($p<0.001$ for both comparisons), and neurons of class 1, regardless of area and epoch, showed the overall higher firing rate among the three classes ($p<0.001$ for both comparisons). Significant interaction of Cell class and Area ($F=3.19$, $p=0.013$) indicated that neurons of class 1 exhibit a discharge stronger than that of the other classes ($p<0.05$) in area F6, whereas this tendency is not significant in AIP ($p=0.33$) and F5 ($p=0.38$). The interaction of Area and Epoch ($F=5.58$, $p<0.001$) indicated that F5 neurons' activity was overall facilitated relative to baseline during both object presentation and movement epoch ($p<0.001$ for both comparisons), whereas AIP neurons were significantly facilitated ($p=0.016$) only during object presentation. In turn, area F6 neurons exhibited a significant suppression of their discharge during movement epoch relative to object presentation only ($p=0.023$). Finally, the interaction of Cell class and Epoch ($F=5.52$, $p<0.001$) showed that the overall facilitated response during object presentation appears to be mainly due to the contribution of cells of class 1 ($p<0.001$). These findings are also accounted for by the uneven distribution of facilitated and suppressed neurons in the different classes and areas (Figure 16g).

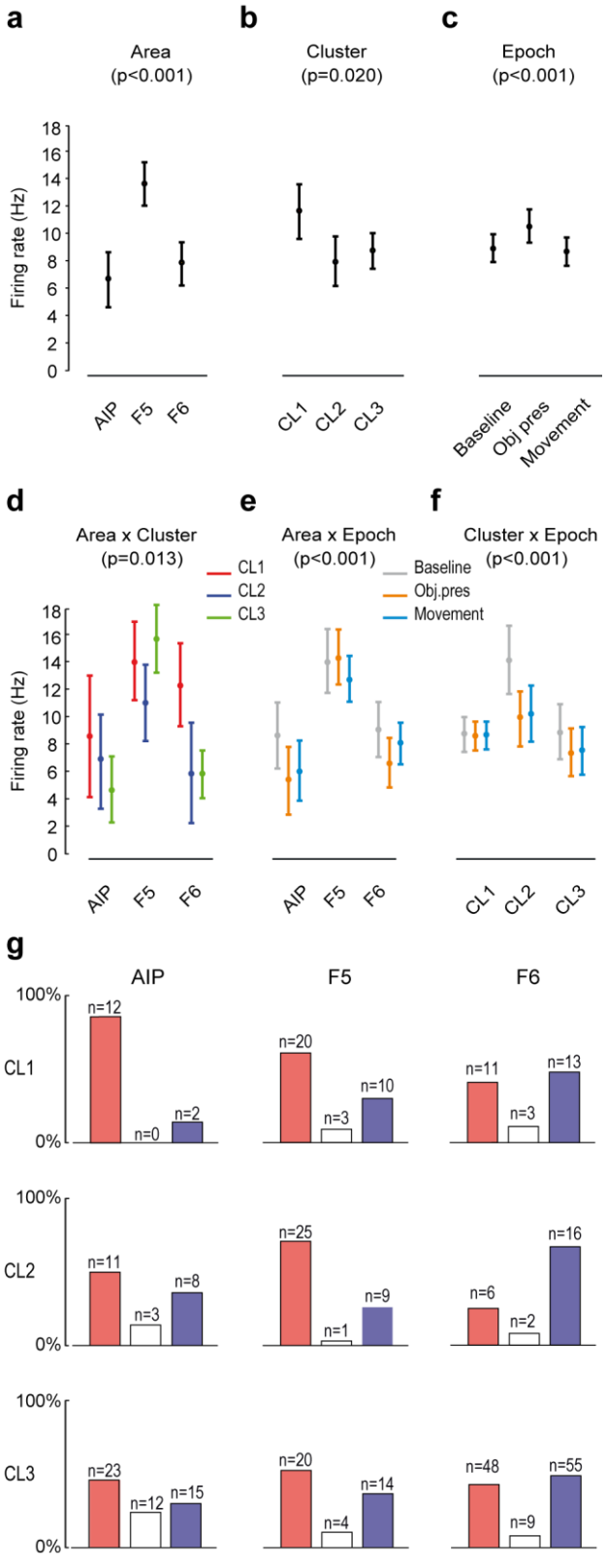

Figure 16. Tuning of different cell classes in different areas during EXE.

(a) Main effect of Area ($F=19.06$, $p<0.001$), indicating that neurons of area F5 have greater firing rate than those of the other two areas (F5-AIP, $p=2\cdot10^{-5}$; F5-F6, $p=9\cdot10^{-6}$), which in turn did not differ from each other ($p=0.34$).

(b) Main effect of Cluster ($F=3.97$, $p=0.0197$), indicating that cells of cluster 1 have greater firing rate than those of the other two clusters (CL1-CL2, $p=0.0008$; CL1-CL3, $p=0.0001$;), which in turn did not differ from each other ($p=0.40$).

(c) Main effect of Epoch ($F=13.17$, $p<0.001$), indicating that there is difference during Object presentation respect the other two epoch.

(d) Interaction between Cluster and Area ($F=3.19$, $p=0.0134$), showing that F5 discharge stronger in cluster 1-2-3 and also cluster 1 of F6 discharge stronger respect cluster 2 and 3

(e) Interaction between Area and Epoch ($F=5.58$, $p<0.001$), indicating that area F5 neurons discharge stronger than those of the other areas in all epochs, including baseline, and their firing rate is higher than baseline during both object presentation ($p=0.043$) and movement ($p=0.032$) epochs; in contrast, AIP neurons significantly increase their firing rate relative to baseline only during object presentation epoch ($p=0.016$), whereas area F6 neurons exhibit an overall suppression of their discharge during movement epoch relative to the object presentation ($p=0.023$).

(f) Interaction between Cluster and Epoch ($F=5.52$, $p<0.001$), indicating that during object presentation epoch cells of cluster 1 show the overall strongest firing rate ($p<0.001$ for all comparisons).

(g) Percentage of facilitated (red), suppressed (blue) and non-significant (white) neurons within areas and cell classes in EXE.

The same analysis applied to the response of the three neuronal classes recorded from the three areas during OBS (Figure 15d) yielded similar results. In particular (Figure 17), the effect of Area ($F=26.06$, $p<0.001$) indicated that neurons of area F5 showed the strongest firing rate among the three areas ($p<0.001$ for both comparisons), which in turn did not differ from each other. Interaction of Area and Epoch ($F=7.25$, $p<0.001$) revealed that F5 exhibited an overall facilitated response during action observation, which was significantly stronger that both baseline ($p<0.001$) and object presentation ($p<0.001$), which in turn did not differ from each other ($p=0.3$). Furthermore, the interaction between Cell class and Epoch ($F=3.79$, $p=0.0047$) showed that cells belonging to class 1 exhibited overall greater firing rate relative to the other classes, with exception of class 2 during baseline and movement epoch. The relatively lower differences in firing rate during OBS as compared to EXE are likely accounted for by the greater modulatory influence exerted by neurons with inhibited response (Figure 17e), which may play a role in balancing the overall motor output during action observation (A Kraskov et al. 2014).

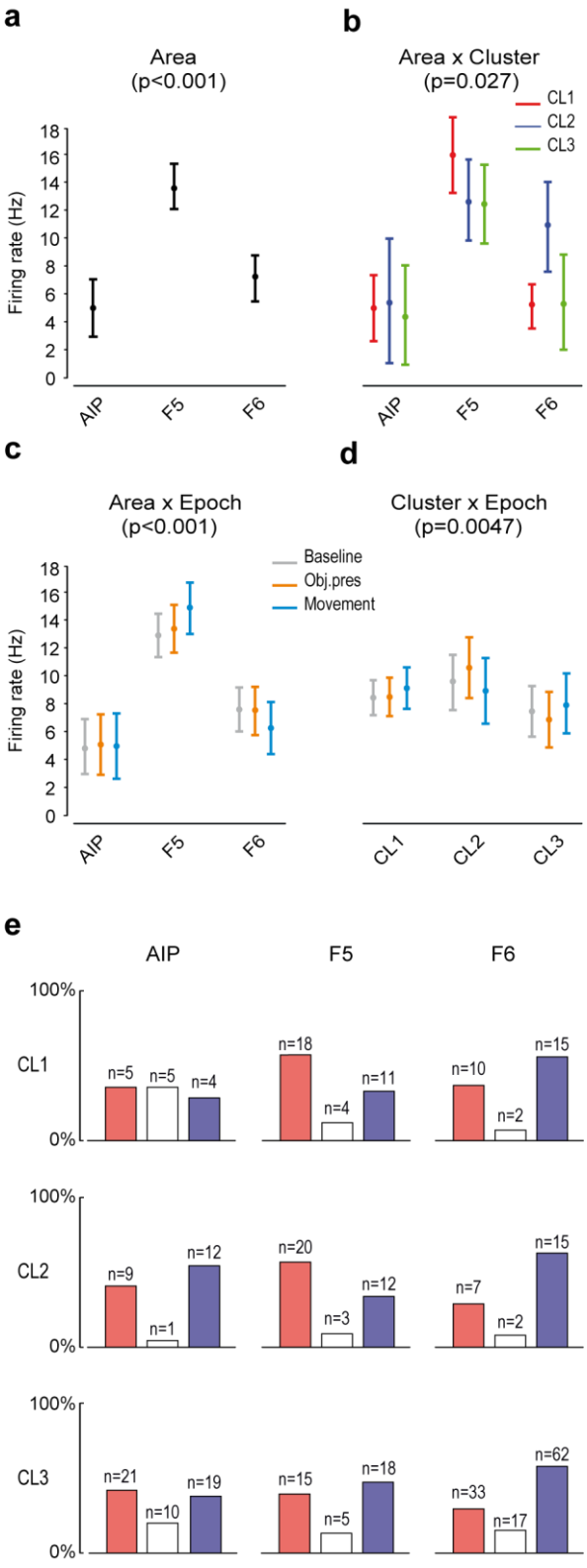

Figure 17. Tuning of different cell classes in different areas during OBS.

(a) Main effect of Area (F=26.06, p<0.001), indicating that neurons of area F5 have greater firing rate than those of the other two areas (F5-AIP, $p=2\cdot10^{-5}$; F5-F6, $p=9\cdot10^{-6}$), which in turn did not differ from each other (p=0.31).

(b) Interaction between Cluster and Area (F=2.77, p=0.0134), showing that F5 have stronger discharge respect the other two areas in cluster 1,2 and 3.

(c) Interaction between Area and Epoch (F=7.25, p<0.001), indicating that area F5 neurons discharge stronger than those of the other areas in all epochs, including baseline, but their firing rate during action observation is higher than baseline (p<0.001) and object presentation (p<0.001), which in turn did not differ from each other (p=0.3); in contrast, the other two areas do not show a significant modulation in the firing rate of their neurons considered altogether.

(d) Interaction between Cluster and Epoch (F=3.79, p<0.005), indicating that during object presentation epoch, cells of cluster 1 show a magnitude of firing rate significantly greater (p<0.05) than all comparisons except baseline and movement epoch of cells in cluster 2.

(e) Percentage of facilitated (red), suppressed (blue) and non-significant (white) neurons within areas and cell classes in OBS.

As a final step, we asked whether individual neurons' modulation during the movement epoch of EXE and OBS varied depending on area and cell class. Indeed, the only available evidence concern pyramidal tract neurons of the ventral premotor (Kraskov et al. 2009) and primary motor (Vigneswaran et al. 2011) cortex. To address this issue in our data set, we devised an index to compute the Mutual Modulation Depth (MMD) of individual neurons' discharge during EXE and OBS by computing (bin-by-bin) the product of EXE and OBS net normalized activity (see Methods). MMD values of a neuron's response in the two tasks are all the more positive as greater is the positive (Figure 18a) or negative (Figure 18b) mutual modulation and all the more negative as greater is the opposite positive-negative modulation (Figure 18c, d); MMD assumes values close to zero whenever a neuron's discharge shows no modulation in any (Figure 18e, f) or both of the tasks. Interestingly, by calculating MMD along tasks unfolding for all the neurons in each cell class of each area during action execution and observation, we found significantly greater MMD for cell class 1 and 2 following movement onset, particularly in AIP and F5, whereas neurons of cell class 3 did not show any significant MMD change during task unfolding, with the exception of cell class 3 of F5, which increases its MMD modulation later on, during object pulling. These findings indicate that, with the partial exception of F5, neurons with stronger mutual modulation during action execution and observation are most often narrow spiking neurons.

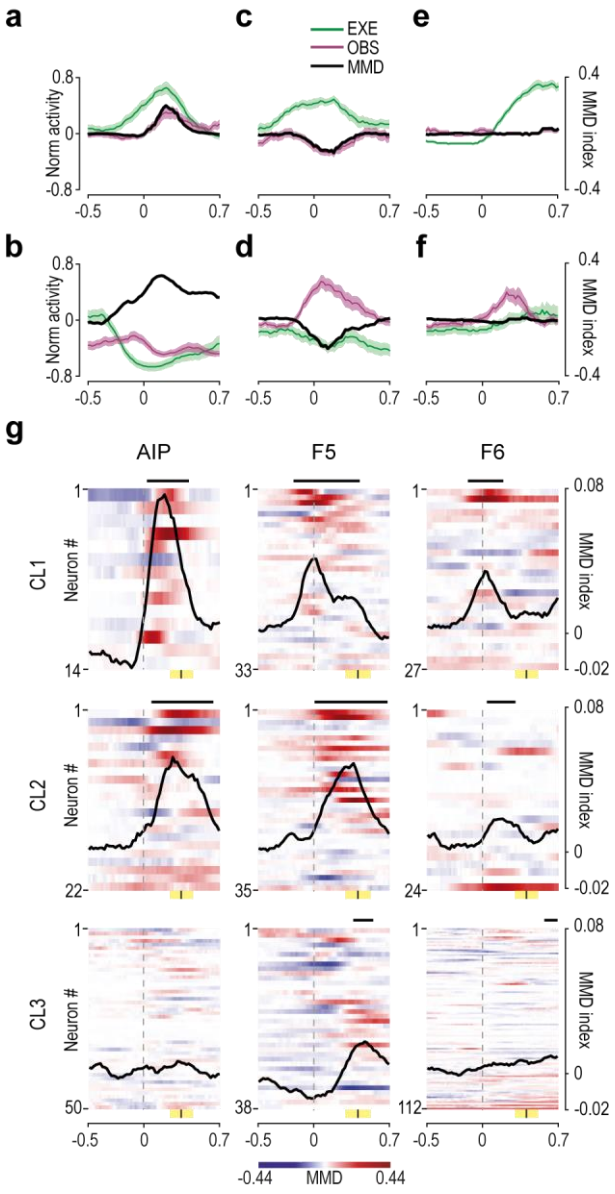

Figure 18. Functional relationship between EXE and OBS within cell classes and areas.
(a-f) Example of neurons showing a positive (a,b), negative (c,d), or null (e,f) MMD index during the movement Epoch. Black curves represent MMD time course, and colored trace represent the average ± standard error net soft-normalized firing rates aligned to movement onset for EXE and OBS.
(g) Heatmap show the MMD time course for each neuron within areas and cell class; black curves represent the average MMD values. Neurons are ordered based on the magnitude of their EXE activity with respect to baseline. Yellow marks represent average ± standard deviation of pull.

7. Discussions

In this study, we recorded single-neuron activity from three crucial nodes of the AON, the intraparietal area AIP and the premotor areas F5 and F6, during the execution and observation of reaching-grasping actions in a Go/No-go paradigm. By leveraging the very same tasks in all areas, we could provide comparative evidence of areal specificities at the system-level and, at the same time, dissect the cell-class coding principles that contribute to the AON functioning.

During the execution task, AIP and F5 showed greater reciprocal similarities with respect to F6. Indeed, they shared a prevalence of facilitated neurons and a greater temporal coupling in their peak of activity and magnitude of selectivity for the target during object presentation and reaching-grasping execution with respect to F6. In contrast, F6 displayed a prevalence of suppressed neurons and a unique contextual selectivity for the Go/No-go cue even prior to target object presentation (Livi et al. 2019), which was absent in the other areas. In addition, F6 also showed a lower and later selectivity for the type of object with respect to AIP and F5. These results support a tight coupling of AIP and F5 in the visuomotor processing of objects for grasping (Dann et al. 2016; Schaffelhofer and Scherberger 2016) and show, in addition, that area F6 strongly differs in terms of timing and strength of its object- and action-related tuning, likely contributing to signal whether a forthcoming action will be performed or withheld.

During the observation task, population response in all areas showed weaker modulations relative to the execution condition, mostly because of a greater number of neurons with suppressed discharge, with the notable exception of F5. In fact, in F5 facilitated responses prevailed also during action observation and decoding analyses evidenced greater and earlier information about other's action with respect to AIP and F6. Notably, as shown by previous studies in F6 (Livi et al. 2019) and, partly, in F5 (Bonini et al. 2014a), we did not observed significant decoding accuracy for the type of object/grip in the observation task in any of the investigated areas, including AIP. This may appear in contrast with some previous evidence of object/grip visual selectivity in parietal (Maeda et al. 2015) and frontal (Papadourakis and Raos 2017; Mazurek et al. 2018) nodes of the AON. However, this apparent discrepancy may be explained by the fact that, in our task, the monkey was required to keep fixation and the observed action

occurred in a fully extrapersonal space sector. These factors, particularly the spatial constraints (Maranesi et al. 2015), are known to reduce or abolish neural selectivity for observed objects. Thus, our findings support the idea that the nodes of the AON here investigated provide a broad signal about the temporal aspects of others' observed actions. Importantly, control analyses on the temporal priority of F5 over the other two areas confirmed its capacity to actively generate a signal that not only anticipates the onset of another's observed action (Maranesi et al. 2014), but it is also independent from the signal coming (260 ms later) from AIP or F6. Previous studies demonstrated that F5 neurons can internally generate representations of external events even with limited (Umiltà et al. 2001; Caggiano et al. 2016; Mazurek et al. 2018) or no (Bonini et al. 2014a) visual information. In a predictive coding framework (Kilner et al. 2007; Shipp et al. 2013), the present findings suggest that among the tight reciprocal connections between F5, AIP and F6 (Borra et al. 2008; Bruni et al. 2018; Lanzilotto et al. 2019; Albertini et al. 2020), the projections carrying predictive signals from area F5 have an overriding functional relevance in triggering neuronal activity at all levels of the network relative to feedforward information coming from visual areas, at least in highly predictable contexts.

Is there any differential contribution of functionally distinct cell classes on areal specificities in the AON? So far, the only available evidence was constituted by two studies demonstrating that a set of antidromically-identified pyramidal-tract neurons in F5 (Kraskov et al. 2009) and F1 (Vigneswaran et al. 2013) exhibit mirror properties, more than half showing suppressed activity during action observation. In the present study, we applied recently validated methods to perform an unbiased clustering of single neuron waveforms, blind to the area of origin (Trainito et al. 2019), and obtained three neuronal classes. These classes varied in terms of their spike width from narrow spiking (class 1) to broadly spiking (class 3) neurons (Mitchell et al. 2007; Diester and Nieder 2008; Song and McPeek 2010; Kaufman et al. 2010; Torres-Gomez et al. 2020). By assessing cell class responses in the execution and observation tasks, we found that narrower spiking neurons fired stronger during baseline, object presentation and action execution/observation and showed a more marked tendency to fire in burst relative to broadly spiking neurons, which in turn exhibited slower and more regular firing patterns. These differences between narrow and broad spiking neurons are consistent with those reported by previous studies with different tasks in other cortical areas (Katai et al. 2010; Zhang et al. 2018; Thiele et al. 2016).

Interestingly, we found that area F5 hosts a greater fraction of neurons in the first two classes (narrow spiking), whereas F6 exhibits the opposite trend, with a greater fraction of neurons belonging to class 3. Thus, assuming that the fraction of putative interneurons, which are deemed to exhibit mainly narrow spikes (but see also Zaitsev et al. 2009), is uniform across areas, the greater fraction of narrow spiking neurons in F5 may be due to a greater presence of relatively large pyramidal neurons (Belmalih et al. 2008), which can exhibit thin spikes as well (Vigneswaran et al. 2011), and to the acute recording approach applied to this area (Bonini et al. 2014a), which likely produces a sampling bias toward bigger cell bodies. In turn, the greater fraction of neurons belonging to class 3 in area F6 may be due to the greater presence, in this agranular rostral premotor area, of many medium-to-small size pyramidal neurons (Matsuzaka et al.1992).

One of the most relevant findings about the relationship between areal specificities and cell classes concerns the shared motor and sensory processing of self and others' action, which is operated by narrower spiking neurons (class 1 and 2), especially of areas AIP and F5, whereas broadly spiking neurons (class 3) encode more specifically either self- or other-related information. Although previous findings challenged the possibility to reliably dissociate interneurons from pyramidal neurons solely based on extracellular spike shape (Zaitsev et al. 2009), many extrcellular recording studies in monkeys suggest that narrower spiking neurons most likely correspond to interneurons whereas broadly spiking neurons to pyramidal cells (Kaufman et al. 2010), with the notable exception of motor and premotor cortex where particularly large pyramidal cells can show extremely narrow spikes (Vigneswaran et al. 2011). Although admittedly speculative, the present and previous findings suggest the fascinating possibility that mutual visual and motor representations of actions of self and other, which is typical of neurons with mirror properties (Bonini 2017), involves a considerable set of local interneurons in all the investigated nodes of the AON (in addition to pyramidal cells), and especially in the parieto-frontal circuit involving AIP and F5. In contrast, long range cortico-cortical and corticofugal connections may rely on mostly unimodal (visual or motor) projections of small-to-medium size pyramidal neurons. In line with this hypothesis, a previous study (Kraskov et al. 2009) reported that suppression of activity in F5 may be significantly more common among PTNs compared with unidentified neurons: because in the data set of these authors possible interneurons could only be present among the unidentified neuronal data set, this finding support the idea that a sizable fraction of neurons with jointly facilitated response during execution and observation of actions are inhibitory

interneurons. In this view, these “mirror interneurons” could represent efference copies of motor actions (Bonini 2017) as previously shown in songbirds (Prather et al. 2008), likely playing a role in shaping social responses or in producing the previously observed suppression of discharge of pyramidal (especially corticospinal) neurons.

In summary, our findings shed light on the comparative properties of three of the recently recognized main nodes of the AON in the monkey, providing new evidence on local areal specificities and the possible underlying cell class mechanisms, which are impossible to investigate in human subjects. The results allowed us to support precise hypothesis on the intrinsic cellular machinery underlying cortical processing of self and others’ action that, if confirmed, may considerably advance our understanding of the wide range of perceptual and socio-cognitive functions played by the cortical motor system.

8. Reference:

Albertini, Davide, Marzio Gerbella, Marco Lanzilotto, Alessandro Livi, Monica Maranesi, Carolina Giulia Ferroni, and Luca Bonini. 2020. "Connectional Gradients Underlie Functional Transitions in Monkey Pre-Supplementary Motor Area." *Progress in Neurobiology* 184: 101699. https://doi.org/https://doi.org/10.1016/j.pneurobio.2019.101699.

Ardid, Salva, Martin Vinck, Daniel Raping, Susanna Marquez, Stefan Everling, and Thilo Womelsdorf. 2015. "Mapping of Functionally Characterized Cell Classes onto Canonical Circuit Operations in Primate Prefrontal Cortex." *Journal of Neuroscience* 35 (7): 2975–91. https://doi.org/10.1523/JNEUROSCI.2700-14.2015.

Barthó, Peter, Hajime Hirase, Lenaïc Monconduit, Michael Zugaro, Kenneth D Harris, and György Buzsáki. 2004. "Characterization of Neocortical Principal Cells and Interneurons by Network Interactions and Extracellular Features." *Journal of Neurophysiology* 92 (1): 600–608. https://doi.org/10.1152/jn.01170.2003.

Barz, F., A. Livi, M. Lanzilotto, M. Maranesi, L. Bonini, O. Paul, and P. Ruther. 2017. "Versatile, Modular 3D Microelectrode Arrays for Neuronal Ensemble Recordings: From Design to Fabrication, Assembly, and Functional Validation in Non-Human Primates." *Journal of Neural Engineering* 14 (3). https://doi.org/10.1088/1741-2552/aa5a90.

Belmalih, Abdelouahed, Elena Borra, Massimo Contini, Marzio Gerbella, Stefano Rozzi, and Giuseppe Luppino. 2008. "Multimodal Architectonic Subdivision of the Rostral Part (Area F5) of the Macaque Ventral Premotor Cortex." *Journal of Comparative Neurology* 512 (2): 183–217. https://doi.org/10.1002/cne.21892.

Bonini, L., M. Maranesi, A. Livi, L. Fogassi, and G. Rizzolatti. 2014. "Space-Dependent Representation of Objects and Other's Action in Monkey Ventral Premotor Grasping Neurons." *Journal of Neuroscience* 34 (11): 4108–19. https://doi.org/10.1523/JNEUROSCI.4187-13.2014.

Bonini, Luca. 2017. "The Extended Mirror Neuron Network: Anatomy, Origin, and Functions." *The Neuroscientist* 23 (1): 56–67. https://doi.org/10.1177/1073858415626400.

Bonini, Luca, Monica Maranesi, Alessandro Livi, Leonardo Fogassi, and Giacomo Rizzolatti. 2014a. "Ventral Premotor Neurons Encoding Representations of Action during Self and Others' Inaction." *Current Biology* 24 (14): 1611–14. https://doi.org/10.1016/j.cub.2014.05.047.

Bonini, Luca, Monica Maranesi, Alessandro Livi, Leonardo Fogassi, and Giacomo Rizzolatti. 2014b. "Space-Dependent Representation of Objects and Other's Action in Monkey Ventral Premotor Grasping Neurons." *The Journal of Neuroscience* 34 (11): 4108 LP – 4119. http://www.jneurosci.org/content/34/11/4108.abstract.

Bonini, Luca, Stefano Rozzi, Francesca Ugolotti Serventi, Luciano Simone, Pier F Ferrari, and Leonardo Fogassi. 2009. "Ventral Premotor and Inferior Parietal Cortices Make Distinct Contribution to Action Organization and Intention Understanding." *Cerebral Cortex* 20 (6): 1372–85. https://doi.org/10.1093/cercor/bhp200.

Borra, Elena, Abdelouahed Belmalih, Roberta Calzavara, Marzio Gerbella, Akira Murata, Stefano Rozzi, and Giuseppe Luppino. 2008. "Cortical Connections of the Macaque Anterior Intraparietal (AIP) Area." *Cerebral Cortex* 18 (5): 1094–1111. https://doi.org/10.1093/cercor/bhm146.

Borra, Elena, Marzio Gerbella, Stefano Rozzi, and Giuseppe Luppino. 2017. "The Macaque Lateral Grasping Network: A Neural Substrate for Generating Purposeful Hand Actions." *Neuroscience & Biobehavioral Reviews* 75: 65–90.

https://doi.org/https://doi.org/10.1016/j.neubiorev.2017.01.017.

Breveglieri, R, M De Vitis, K Hadjidimitrakis, C Galletti, and P Fattori. 2019. “Processing of Depth and Direction Signals in the Medial Posterior Parietal Cortex of the Macaque.” In *ACTA PHYSIOLOGICA*, 227:65. WILEY 111 RIVER ST, HOBOKEN 07030-5774, NJ USA.

Bruni, Stefania, Marzio Gerbella, Luca Bonini, Elena Borra, Gino Coudé, Pier Francesco Ferrari, Leonardo Fogassi, et al. 2018. “Cortical and Subcortical Connections of Parietal and Premotor Nodes of the Monkey Hand Mirror Neuron Network.” *Brain Structure and Function* 223 (4): 1713–29. https://doi.org/10.1007/s00429-017-1582-0.

Bruni, Stefania, Valentina Giorgetti, Leonardo Fogassi, and Luca Bonini. 2015. “Multimodal Encoding of Goal-Directed Actions in Monkey Ventral Premotor Grasping Neurons.” *Cerebral Cortex* 27 (1): 522–33. https://doi.org/10.1093/cercor/bhv246.

Caggiano, Vittorio, Falk Fleischer, Joern K Pomper, Martin A Giese, and Peter Thier. 2016. “Mirror Neurons in Monkey Premotor Area F5 Show Tuning for Critical Features of Visual Causality Perception.” *Current Biology* 26 (22): 3077–82. https://doi.org/https://doi.org/10.1016/j.cub.2016.10.007.

Caggiano, Vittorio, Leonardo Fogassi, Giacomo Rizzolatti, Joern K Pomper, Peter Thier, Martin A Giese, and Antonino Casile. 2011. “View-Based Encoding of Actions in Mirror Neurons of Area F5 in Macaque Premotor Cortex.” *Current Biology* 21 (2): 144–48. https://doi.org/https://doi.org/10.1016/j.cub.2010.12.022.

Caggiano, Vittorio, Martin Giese, Peter Thier, and Antonino Casile. 2015. “Encoding of Point of View during Action Observation in the Local Field Potentials of Macaque Area F5.” *European Journal of Neuroscience* 41 (4): 466–76. https://doi.org/10.1111/ejn.12793.

Caminiti, Roberto, Elena Borra, Federica Visco-Comandini, Alexandra Battaglia-Mayer, Bruno B Averbeck, and Giuseppe Luppino. 2017. “Computational Architecture of the Parieto-Frontal Network Underlying Cognitive-Motor Control in Monkeys.” *Eneuro* 4 (1): ENEURO.0306-16.2017. https://doi.org/10.1523/ENEURO.0306-16.2017.

Carmichael, S T, and J L Price. 1994. “Architectonic Subdivision of the Orbital and Medial Prefrontal Cortex in the Macaque Monkey.” *Journal of Comparative Neurology* 346 (3): 366–402. https://doi.org/10.1002/cne.903460305.

Chang, Steve W C, Anthony R Dickinson, and Lawrence H Snyder. 2008. “Limb-Specific Representation for Reaching in the Posterior Parietal Cortex.” *The Journal of Neuroscience : The Official Journal of the Society for Neuroscience* 28 (24): 6128–40. https://doi.org/10.1523/JNEUROSCI.1442-08.2008.

Chung, Jason E., Jeremy F. Magland, Alex H. Barnett, Vanessa M. Tolosa, Angela C. Tooker, Kye Y. Lee, Kedar G. Shah, Sarah H. Felix, Loren M. Frank, and Leslie F. Greengard. 2017. “A Fully Automated Approach to Spike Sorting.” *Neuron* 95 (6): 1381-1394.e6. https://doi.org/10.1016/j.neuron.2017.08.030.

Cisek, Paul, and John F. Kalaska. 2004. “Neural of Correlates of Mental Rehearsal in Dorsal Premotor Cortex.” *Nature* 431 (7011): 993–96. https://doi.org/10.1038/nature03005.

Cisek, Paul, and John F. Kalaska. 2010. “Neural Mechanisms for Interacting with a World Full of Action Choices.” *Annual Review of Neuroscience* 33 (1): 269–98. https://doi.org/10.1146/annurev.neuro.051508.135409.

Cohen, Jeremiah Y., Pierre Pouget, Richard P. Heitz, Geoffrey F. Woodman, and Jeffrey D. Schall. 2009. “Biophysical Support for Functionally Distinct Cell Types in the Frontal Eye Field.” *Journal of Neurophysiology* 101 (2): 912–16. https://doi.org/10.1152/jn.90272.2008.

Connors, B W, M J Gutnick, and D A Prince. 1982. “Electrophysiological Properties of

Neocortical Neurons in Vitro." *Journal of Neurophysiology* 48 (6): 1302–20. https://doi.org/10.1152/jn.1982.48.6.1302.

Connors, Barry W, and Michael J Gutnick. 1990. "Intrinsic Firing Patterns of Diverse Neocortical Neurons." *Trends in Neurosciences* 13 (3): 99–104. https://doi.org/https://doi.org/10.1016/0166-2236(90)90185-D.

Dann, Benjamin, Jonathan A Michaels, Stefan Schaffelhofer, and Hansjörg Scherberger. 2016. "Uniting Functional Network Topology and Oscillations in the Fronto-Parietal Single Unit Network of Behaving Primates." *ELife* 5 (August): e15719. https://doi.org/10.7554/eLife.15719.

DeFelipe, Javier, and Isabel Fariñas. 1992. "The Pyramidal Neuron of the Cerebral Cortex: Morphological and Chemical Characteristics of the Synaptic Inputs." *Progress in Neurobiology* 39 (6): 563–607. https://doi.org/https://doi.org/10.1016/0301-0082(92)90015-7.

Diester, Ilka, and Andreas Nieder. 2008. "Complementary Contributions of Prefrontal Neuron Classes in Abstract Numerical Categorization." *Journal of Neuroscience* 28 (31): 7737–47. https://doi.org/10.1523/JNEUROSCI.1347-08.2008.

Dushanova, Juliana, and John Donoghue. 2010. "Neurons in Primary Motor Cortex Engaged during Action Observation." *The European Journal of Neuroscience* 31 (2): 386–98. https://doi.org/10.1111/j.1460-9568.2009.07067.x.

Elston, Guy, Ruth Benavides-Piccione, Alejandra Elston, Paul Manger, and Javier Defelipe. 2011. "Pyramidal Cells in Prefrontal Cortex of Primates: Marked Differences in Neuronal Structure Among Species." *Frontiers in Neuroanatomy* 5: 2. https://doi.org/10.3389/fnana.2011.00002.

F., Ferrari P, Bonini L., and Fogassi L. 2009. "From Monkey Mirror Neurons to Primate Behaviours: Possible 'Direct' and 'Indirect' Pathways." *Philosophical Transactions of the Royal Society B: Biological Sciences* 364 (1528): 2311–23. https://doi.org/10.1098/rstb.2009.0062.

Falcone, Rossella, Emiliano Brunamonti, Stefano Ferraina, and Aldo Genovesio. 2016. "Neural Encoding of Self and Another Agent's Goal in the Primate Prefrontal Cortex: Human–Monkey Interactions." *Cerebral Cortex* 26 (12): 4613–22. https://doi.org/10.1093/cercor/bhv224.

Falcone, Rossella, Rossella Cirillo, Stefano Ferraina, and Aldo Genovesio. 2017. "Neural Activity in Macaque Medial Frontal Cortex Represents Others' Choices." *Scientific Reports* 7 (October): 12663. https://doi.org/10.1038/s41598-017-12822-5.

Fattori, Patrizia, Vassilis Raos, Rossella Breveglieri, Annalisa Bosco, Nicoletta Marzocchi, and Claudio Galletti. 2010. "The Dorsomedial Pathway Is Not Just for Reaching: Grasping Neurons in the Medial Parieto-Occipital Cortex of the Macaque Monkey." *The Journal of Neuroscience* 30 (1): 342 LP – 349. https://doi.org/10.1523/JNEUROSCI.3800-09.2010.

Ferroni, C.G., M. Maranesi, A. Livi, M. Lanzilotto, and L. Bonini. 2017. "Comparative Performance of Linear Multielectrode Probes and Single-Tip Electrodes for Intracortical Microstimulation and Single-Neuron Recording in Macaque Monkey." *Frontiers in Systems Neuroscience* 11. https://doi.org/10.3389/fnsys.2017.00084.

Fiave, Prosper Agbesi, Saloni Sharma, Jan Jastorff, and Koen Nelissen. 2018. "Investigating Common Coding of Observed and Executed Actions in the Monkey Brain Using Cross-Modal Multi-Variate FMRI Classification." *NeuroImage* 178: 306–17. https://doi.org/https://doi.org/10.1016/j.neuroimage.2018.05.043.

Fogassi, Leonardo, Pier Francesco Ferrari, Benno Gesierich, Stefano Rozzi, Fabian Chersi, and Giacomo Rizzolatti. 2005. “Parietal Lobe: From Action Organization to Intention Understanding.” *Science* 308 (5722): 662 LP – 667. https://doi.org/10.1126/science.1106138.

Fogassi, Leonardo, Vittorio Gallese, Giovanni Buccino, Laila Craighero, Luciano Fadiga, and Giacomo Rizzolatti. 2001. “Cortical Mechanism for the Visual Guidance of Hand Grasping Movements in the Monkey: A Reversible Inactivation Study.” *Brain* 124 (3): 571–86. https://doi.org/10.1093/brain/124.3.571.

Gabbott, Paul L A, and Sarah J Bacon. 1996. “Local Circuit Neurons in the Medial Prefrontal Cortex (Areas 24a,b,c, 25 and 32) in the Monkey: I. Cell Morphology and Morphometrics.” *Journal of Comparative Neurology* 364 (4): 567–608. https://doi.org/10.1002/(SICI)1096-9861(19960122)364:4<567::AID-CNE1>3.0.CO;2-1.

Gabbott, Paul L A, Brian G M Dickie, R Roy Vaid, Anthony J N Headlam, and Sarah J Bacon. 1997. “Local-Circuit Neurones in the Medial Prefrontal Cortex (Areas 25, 32 and 24b) in the Rat: Morphology and Quantitative Distribution.” *Journal of Comparative Neurology* 377 (4): 465–99. https://doi.org/10.1002/(SICI)1096-9861(19970127)377:4<465::AID-CNE1>3.0.CO;2-0.

Gallese, Vittorio, Luciano Fadiga, Leonardo Fogassi, and Giacomo Rizzolatti. 1996. “Action Recognition in the Premotor Cortex.” *Brain : A Journal of Neurology* 119 (Pt 2 (2): 593–609. https://doi.org/10.1093/brain/119.2.593.

Gallese, Vittorio, Pier Francesco Ferrari, and Maria Alessandra Umiltà. 2002. “The Mirror Matching System: A Shared Manifold for Intersubjectivity.” *Behavioral and Brain Sciences* 25 (1): 35–36. https://doi.org/DOI: 10.1017/S0140525X02370018.

Gallese, Vittorio, Akira Murata, Masakazu Kaseda, Nanako Niki, and Hideo Sakata. 1994. “Deficit of Hand Preshaping after Muscimol Injection in Monkey Parietal Cortex.” *NeuroReport* 5 (12). https://journals.lww.com/neuroreport/Fulltext/1994/07000/Deficit_of_hand_preshaping_after_muscimol.29.aspx.

Gardner, Esther P, K Srinivasa Babu, Shari D Reitzen, Soumya Ghosh, Alice S Brown, Jessie Chen, Anastasia L Hall, Michael D Herzlinger, Jane B Kohlenstein, and Jin Y Ro. 2007. “Neurophysiology of Prehension. I. Posterior Parietal Cortex and Object-Oriented Hand Behaviors.” *Journal of Neurophysiology* 97 (1): 387–406. https://doi.org/10.1152/jn.00558.2006.

Gerbella, Marzio, Stefano Rozzi, and Giacomo Rizzolatti. 2017. “The Extended Object-Grasping Network.” *Experimental Brain Research* 235 (10): 2903–16. https://doi.org/10.1007/s00221-017-5007-3.

Gold, Carl, Darrell A. Henze, Christof Koch, and György Buzsáki. 2006. “On the Origin of the Extracellular Action Potential Waveform: A Modeling Study.” *Journal of Neurophysiology* 95 (5): 3113–28. https://doi.org/10.1152/jn.00979.2005.

González-Burgos, Guillermo, Leonid S. Krimer, Nadya V. Povysheva, German Barrionuevo, and David A. Lewis. 2005. “Functional Properties of Fast Spiking Interneurons and Their Synaptic Connections with Pyramidal Cells in Primate Dorsolateral Prefrontal Cortex.” *Journal of Neurophysiology* 93 (2): 942–53. https://doi.org/10.1152/jn.00787.2004.

Gray, Charles M, and David A McCormick. 1996. “Chattering Cells: Superficial Pyramidal Neurons Contributing to the Generation of Synchronous Oscillations in the Visual Cortex.” *Science* 274 (5284): 109 LP – 113. https://doi.org/10.1126/science.274.5284.109.

Härtig, Wolfgang, Amin Derouiche, Klaus Welt, Kurt Brauer, Jens Grosche, Michael Mäder, Andreas Reichenbach, and Gert Brückner. 1999. “Cortical Neurons Immunoreactive for the Potassium Channel Kv3.1b Subunit Are Predominantly Surrounded by Perineuronal Nets Presumed as a Buffering System for Cations.” *Brain Research* 842 (1): 15–29. https://doi.org/https://doi.org/10.1016/S0006-8993(99)01784-9.

Henze, Darrell A, Zsolt Borhegyi, Jozsef Csicsvari, Akira Mamiya, Kenneth D Harris, and György Buzsáki. 2000. “Intracellular Features Predicted by Extracellular Recordings in the Hippocampus In Vivo.” *Journal of Neurophysiology* 84 (1): 390–400. https://doi.org/10.1152/jn.2000.84.1.390.

Hepp-Reymond, M.-C., E J Hüsler, M A Maier, and H.-X. Qi. 1994. “Force-Related Neuronal Activity in Two Regions of the Primate Ventral Premotor Cortex.” *Canadian Journal of Physiology and Pharmacology* 72 (5): 571–79. https://doi.org/10.1139/y94-081.

Homayoun, Houman, and Bita Moghaddam. 2007. “NMDA Receptor Hypofunction Produces Opposite Effects on Prefrontal Cortex Interneurons and Pyramidal Neurons.” *Journal of Neuroscience* 27 (43): 11496–500. https://doi.org/10.1523/JNEUROSCI.2213-07.2007.

Hussar, Cory R, and Tatiana Pasternak. 2009. “Flexibility of Sensory Representations in Prefrontal Cortex Depends on Cell Type.” *Neuron* 64 (5): 730–43. https://doi.org/https://doi.org/10.1016/j.neuron.2009.11.018.

Jeannerod, M, M A Arbib, G Rizzolatti, and H Sakata. 1995. “Grasping Objects: The Cortical Mechanisms of Visuomotor Transformation.” *Trends in Neurosciences* 18 (7): 314–20. https://doi.org/https://doi.org/10.1016/0166-2236(95)93921-J.

Jellema, T, C I Baker, B Wicker, and D I Perrett. 2000. “Neural Representation for the Perception of the Intentionality of Actions.” *Brain and Cognition* 44 (2): 280–302. https://doi.org/https://doi.org/10.1006/brcg.2000.1231.

Jellema, Tjeerd, and David I Perrett. 2003. “Perceptual History Influences Neural Responses to Face and Body Postures.” *Journal of Cognitive Neuroscience* 15 (7): 961–71. https://doi.org/10.1162/089892903770007353.

Johnston, Kevin, Joseph F.X. DeSouza, and Stefan Everling. 2009. “Monkey Prefrontal Cortical Pyramidal and Putative Interneurons Exhibit Differential Patterns of Activity between Prosaccade and Antisaccade Tasks.” *Journal of Neuroscience* 29 (17): 5516–24. https://doi.org/10.1523/JNEUROSCI.5953-08.2009.

Katai, Satoshi, Keichiro Kato, Shunpei Unno, Youngnam Kang, Masanori Saruwatari, Naoki Ishikawa, Masato Inoue, and Akichika Mikami. 2010. “Classification of Extracellularly Recorded Neurons by Their Discharge Patterns and Their Correlates with Intracellularly Identified Neuronal Types in the Frontal Cortex of Behaving Monkeys.” *European Journal of Neuroscience* 31 (7): 1322–38. https://doi.org/10.1111/j.1460-9568.2010.07150.x.

Kaufman, Matthew T, Mark M Churchland, Gopal Santhanam, Byron M Yu, Afsheen Afshar, Stephen I Ryu, and Krishna V Shenoy. 2010. “Roles of Monkey Premotor Neuron Classes in Movement Preparation and Execution.” *Journal of Neurophysiology* 104 (2): 799–810. https://doi.org/10.1152/jn.00231.2009.

Kaufman, Matthew T, Mark M Churchland, and Krishna V Shenoy. 2013. “The Roles of Monkey M1 Neuron Classes in Movement Preparation and Execution.” *Journal of Neurophysiology* 110 (4): 817–25. https://doi.org/10.1152/jn.00892.2011.

Kawaguchi, Y, and Y Kubota. 1997. “GABAergic Cell Subtypes and Their Synaptic Connections in Rat Frontal Cortex.” *Cerebral Cortex* 7 (6): 476–86. https://doi.org/10.1093/cercor/7.6.476.

Kawaguchi, Yasuo, Charles J Wilson, Sarah J Augood, and Piers C Emson. 1995. “Striatal Interneurones: Chemical, Physiological and Morphological Characterization.” *Trends in Neurosciences* 18 (12): 527–35.

Kilner, J M, and R N Lemon. 2013. “What We Know Currently about Mirror Neurons.” *Current Biology* 23 (23): R1057–62. https://doi.org/https://doi.org/10.1016/j.cub.2013.10.051.

Kilner, James M, Karl J Friston, and Chris D Frith. 2007. “Predictive Coding: An Account of the Mirror Neuron System.” *Cognitive Processing* 8 (3): 159–66. https://doi.org/10.1007/s10339-007-0170-2.

Kohler, Evelyne, Christian Keysers, M Alessandra Umiltà, Leonardo Fogassi, Vittorio Gallese, and Giacomo Rizzolatti. 2002. “Hearing Sounds, Understanding Actions: Action Representation in Mirror Neurons.” *Science* 297 (5582): 846 LP – 848. https://doi.org/10.1126/science.1070311.

Kraskov, A, R Philipp, S Waldert, G Vigneswaran, M M Quallo, and R N Lemon. 2014. “Corticospinal Mirror Neurons.” *Philosophical Transactions of the Royal Society of London. Series B, Biological Sciences* 369 (1644): 20130174. https://doi.org/10.1098/rstb.2013.0174.

Kraskov, Alexander, Numa Dancause, Marsha M Quallo, Samantha Shepherd, and Roger N Lemon. 2009. “Corticospinal Neurons in Macaque Ventral Premotor Cortex with Mirror Properties: A Potential Mechanism for Action Suppression?” *Neuron* 64 (6): 922–30. https://doi.org/https://doi.org/10.1016/j.neuron.2009.12.010.

Krimer, Leonid S., Aleksey V. Zaitsev, Gabriela Czanner, Sven Kröner, Guillermo González-Burgos, Nadezhda V. Povysheva, Satish Iyengar, German Barrionuevo, and David A. Lewis. 2005. “Cluster Analysis-Based Physiological Classification and Morphological Properties of Inhibitory Neurons in Layers 2-3 of Monkey Dorsolateral Prefrontal Cortex.” *Journal of Neurophysiology* 94 (5): 3009–22. https://doi.org/10.1152/jn.00156.2005.

Kurata, K, and J Tanji. 1986. “Premotor Cortex Neurons in Macaques: Activity before Distal and Proximal Forelimb Movements.” *The Journal of Neuroscience* 6 (2): 403 LP – 411. https://doi.org/10.1523/JNEUROSCI.06-02-00403.1986.

Lanzilotto, M, M Gerbella, V Perciavalle, and C Lucchetti. 2017. “Neuronal Encoding of Self and Others’ Head Rotation in the Macaque Dorsal Prefrontal Cortex.” *Scientific Reports* 7 (1): 8571. https://doi.org/10.1038/s41598-017-08936-5.

Lanzilotto, Marco, Carolina Giulia Ferroni, Alessandro Livi, Marzio Gerbella, Monica Maranesi, Elena Borra, Lauretta Passarelli, et al. 2019. “Erratum: Anterior Intraparietal Area: A Hub in the Observed Manipulative Action Network.” *Cerebral Cortex* 30 (1): 100. https://doi.org/10.1093/cercor/bhz074.

Lanzilotto, Marco, Alessandro Livi, Monica Maranesi, Marzio Gerbella, Falk Barz, Patrick Ruther, Leonardo Fogassi, Giacomo Rizzolatti, and Luca Bonini. 2016. “Extending the Cortical Grasping Network: Pre-Supplementary Motor Neuron Activity During Vision and Grasping of Objects.” *Cerebral Cortex* 26 (12): 4435–49. http://dx.doi.org/10.1093/cercor/bhw315.

Lanzilotto, Marco, Monica Maranesi, Alessandro Livi, Carolina Giulia Ferroni, Guy A Orban, and Luca Bonini. 2020. “Stable Readout of Observed Actions from Format-Dependent Activity of Monkey’s Anterior Intraparietal Neurons.” *Proceedings of the National Academy of Sciences*, June, 202007018. https://doi.org/10.1073/pnas.2007018117.

Livi, Alessandro, Carolina Giulia Ferroni, Elena Borra, Leonardo Fogassi, Luca Bonini, Marzio Gerbella, Monica Maranesi, et al. 2019. “Anterior Intraparietal Area: A Hub in the Observed Manipulative Action Network.” *Cerebral Cortex* 29 (4): 1816–33. https://doi.org/10.1093/cercor/bhz011.

Livi, Alessandro, Marco Lanzilotto, Monica Maranesi, Leonardo Fogassi, Giacomo Rizzolatti, and Luca Bonini. 2019. “Agent-Based Representations of Objects and Actions in the Monkey Pre-Supplementary Motor Area.” *Proceedings of the National Academy of Sciences* 116 (7): 2691 LP – 2700. https://doi.org/10.1073/pnas.1810890116.

Luppino, G, M Matelli, R M Camarda, V Gallese, and G Rizzolatti. 1991. “Multiple Representations of Body Movements in Mesial Area 6 and the Adjacent Cingulate Cortex: An Intracortical Microstimulation Study in the Macaque Monkey.” *Journal of Comparative Neurology* 311 (4): 463–82. https://doi.org/10.1002/cne.903110403.

Maeda, Kazutaka, Hiroaki Ishida, Katsumi Nakajima, Masahiko Inase, and Akira Murata. 2015. “Functional Properties of Parietal Hand Manipulation–Related Neurons and Mirror Neurons Responding to Vision of Own Hand Action.” *Journal of Cognitive Neuroscience* 27 (3): 560–72. https://doi.org/10.1162/jocn_a_00742.

Maimon, Gaby, and John A Assad. 2009. “Beyond Poisson: Increased Spike-Time Regularity across Primate Parietal Cortex.” *Neuron* 62 (3): 426–40. https://doi.org/https://doi.org/10.1016/j.neuron.2009.03.021.

Maranesi, Monica, Alessandro Livi, and Luca Bonini. 2015. “Processing of Own Hand Visual Feedback during Object Grasping in Ventral Premotor Mirror Neurons.” *The Journal of Neuroscience* 35 (34): 11824 LP – 11829. https://doi.org/10.1523/JNEUROSCI.0301-15.2015.

Maranesi, Monica, Alessandro Livi, Leonardo Fogassi, Giacomo Rizzolatti, and Luca Bonini. 2014. “Mirror Neuron Activation Prior to Action Observation in a Predictable Context.” *The Journal of Neuroscience* 34 (45): 14827 LP – 14832. https://doi.org/10.1523/JNEUROSCI.2705-14.2014.

Maranesi, Monica, Francesca Rodà, Luca Bonini, Stefano Rozzi, Pier Francesco Ferrari, Leonardo Fogassi, and Gino Coudé. 2012. “Anatomo-Functional Organization of the Ventral Primary Motor and Premotor Cortex in the Macaque Monkey.” *European Journal of Neuroscience* 36 (10): 3376–87. https://doi.org/10.1111/j.1460-9568.2012.08252.x.

Markram, Henry, Maria Toledo-Rodriguez, Yun Wang, Anirudh Gupta, Gilad Silberberg, and Caizhi Wu. 2004. “Interneurons of the Neocortical Inhibitory System.” *Nature Reviews Neuroscience* 5 (10): 793–807. https://doi.org/10.1038/nrn1519.

Matsuzaka, Y, H Aizawa, and J Tanji. 1992. “A Motor Area Rostral to the Supplementary Motor Area (Presupplementary Motor Area) in the Monkey: Neuronal Activity during a Learned Motor Task.” *Journal of Neurophysiology* 68 (3): 653–62. https://doi.org/10.1152/jn.1992.68.3.653.

Mazurek, Kevin A, Adam G Rouse, and Marc H Schieber. 2018. “Mirror Neuron Populations Represent Sequences of Behavioral Epochs During Both Execution and Observation.” *The Journal of Neuroscience* 38 (18): 4441 LP – 4455. https://doi.org/10.1523/JNEUROSCI.3481-17.2018.

McCormick, D A, B W Connors, J W Lighthall, and D A Prince. 1985. “Comparative Electrophysiology of Pyramidal and Sparsely Spiny Stellate Neurons of the Neocortex.” *Journal of Neurophysiology* 54 (4): 782–806. https://doi.org/10.1152/jn.1985.54.4.782.

Meyers, Ethan M. 2013. “The Neural Decoding Toolbox.” *Frontiers in Neuroinformatics* 7 (May): 8. https://doi.org/10.3389/fninf.2013.00008.

Mitchell, Jude F, Kristy A Sundberg, and John H Reynolds. 2007. “Differential Attention-Dependent Response Modulation across Cell Classes in Macaque Visual Area V4.” *Neuron* 55 (1): 131–41. https://doi.org/https://doi.org/10.1016/j.neuron.2007.06.018.

Moore, Alexandra K., and Michael Wehr. 2013. “Parvalbumin-Expressing Inhibitory Interneurons in Auditory Cortex Are Well-Tuned for Frequency.” *Journal of Neuroscience* 33 (34): 13713–23. https://doi.org/10.1523/JNEUROSCI.0663-13.2013.

Mountcastle, V B, W H Talbot, H Sakata, and J Hyvärinen. 1969. “Cortical Neuronal Mechanisms in Flutter-Vibration Studied in Unanesthetized Monkeys. Neuronal Periodicity and Frequency Discrimination.” *Journal of Neurophysiology* 32 (3): 452–84. https://doi.org/10.1152/jn.1969.32.3.452.

Mukamel, Roy, Arne D Ekstrom, Jonas Kaplan, Marco Iacoboni, and Itzhak Fried. 2010. “Single-Neuron Responses in Humans during Execution and Observation of Actions.” *Current Biology* 20 (8): 750–56. https://doi.org/https://doi.org/10.1016/j.cub.2010.02.045.

Murata, Akira, Luciano Fadiga, Leonardo Fogassi, Vittorio Gallese, Vassilis Raos, and Giacomo Rizzolatti. 1997. “Object Representation in the Ventral Premotor Cortex (Area F5) of the Monkey.” *Journal of Neurophysiology* 78 (4): 2226–30. https://doi.org/10.1152/jn.1997.78.4.2226.

Murata, Akira, Vittorio Gallese, Giuseppe Luppino, Masakazu Kaseda, and Hideo Sakata. 2000. “Selectivity for the Shape, Size, and Orientation of Objects for Grasping in Neurons of Monkey Parietal Area AIP.” *Journal of Neurophysiology* 83 (5): 2580–2601. https://doi.org/10.1152/jn.2000.83.5.2580.

Nachev, Parashkev, Christopher Kennard, and Masud Husain. 2008. “Functional Role of the Supplementary and Pre-Supplementary Motor Areas.” *Nature Reviews Neuroscience* 9 (11): 856–69. https://doi.org/10.1038/nrn2478.

Nelissen, Koen, Elena Borra, Marzio Gerbella, Stefano Rozzi, Giuseppe Luppino, Wim Vanduffel, Giacomo Rizzolatti, and Guy A Orban. 2011. “Action Observation Circuits in the Macaque Monkey Cortex.” *The Journal of Neuroscience* 31 (10): 3743 LP – 3756. https://doi.org/10.1523/JNEUROSCI.4803-10.2011.

Nowak, Lionel G, Rony Azouz, Maria V Sanchez-Vives, Charles M Gray, and David A McCormick. 2003. “Electrophysiological Classes of Cat Primary Visual Cortical Neurons In Vivo as Revealed by Quantitative Analyses.” *Journal of Neurophysiology* 89 (3): 1541–66. https://doi.org/10.1152/jn.00580.2002.

Pani, Pierpaolo, Tom Theys, Maria C Romero, and Peter Janssen. 2014. “Grasping Execution and Grasping Observation Activity of Single Neurons in the Macaque Anterior Intraparietal Area.” *Journal of Cognitive Neuroscience* 26 (10): 2342–55. https://doi.org/10.1162/jocn_a_00647.

Papadourakis, Vassilis, and Vassilis Raos. 2017. “Neurons in the Macaque Dorsal Premotor Cortex Respond to Execution and Observation of Actions.” *Cerebral Cortex* 29 (10): 4223–37. https://doi.org/10.1093/cercor/bhy304.

Pellegrino, G di, L Fadiga, L Fogassi, V Gallese, and G Rizzolatti. 1992. “Understanding Motor Events: A Neurophysiological Study.” *Experimental Brain Research* 91 (1): 176–80. https://doi.org/10.1007/BF00230027.

Prather, J. F., S. Peters, S. Nowicki, and R. Mooney. 2008. “Precise Auditory-Vocal Mirroring in Neurons for Learned Vocal Communication.” *Nature* 451 (7176): 305–10. https://doi.org/10.1038/nature06492.

Quian Quiroga, Rodrigo, and Stefano Panzeri. 2009. “Extracting Information from Neuronal Populations: Information Theory and Decoding Approaches.” *Nature Reviews Neuroscience* 10 (3): 173–85. https://doi.org/10.1038/nrn2578.

Rao, Srinivas G., Graham V. Williams, and Patricia S. Goldman-Rakic. 1999. “Isodirectional Tuning of Adjacent Interneurons and Pyramidal Cells during Working Memory: Evidence for Microcolumnar Organization in PFC.” *Journal of Neurophysiology* 81 (4): 1903–16. https://doi.org/10.1152/jn.1999.81.4.1903.

Raos, Vassilis, Maria-Alessandra Umiltá, Akira Murata, Leonardo Fogassi, and Vittorio Gallese. 2006. "Functional Properties of Grasping-Related Neurons in the Ventral Premotor Area F5 of the Macaque Monkey." *Journal of Neurophysiology* 95 (2): 709–29. https://doi.org/10.1152/jn.00463.2005.

Rizzolatti, G, R Camarda, L Fogassi, M Gentilucci, G Luppino, and M Matelli. 1988. "Functional Organization of Inferior Area 6 in the Macaque Monkey." *Experimental Brain Research* 71 (3): 491–507. https://doi.org/10.1007/BF00248742.

Rizzolatti, G, M Gentilucci, R M Camarda, V Gallese, G Luppino, M Matelli, and L Fogassi. 1990. "Neurons Related to Reaching-Grasping Arm Movements in the Rostral Part of Area 6 (Area 6aβ)." *Experimental Brain Research* 82 (2): 337–50. https://doi.org/10.1007/BF00231253.

Rizzolatti, Giacomo, Luciano Fadiga, Vittorio Gallese, and Leonardo Fogassi. 1996. "Premotor Cortex and the Recognition of Motor Actions." *Cognitive Brain Research* 3 (2): 131–41. https://doi.org/https://doi.org/10.1016/0926-6410(95)00038-0.

Rizzolatti, Giacomo, Cristiana Scandolara, Massimo Matelli, and Maurizio Gentilucci. 1981. "Afferent Properties of Periarcuate Neurons in Macaque Monkeys. II. Visual Responses." *Behavioural Brain Research* 2 (2): 147–63. https://doi.org/https://doi.org/10.1016/0166-4328(81)90053-X.

Robbins, Ashlee A, Steven E Fox, Gregory L Holmes, Rod C Scott, and Jeremy M Barry. 2013. "Short Duration Waveforms Recorded Extracellularly from Freely Moving Rats Are Representative of Axonal Activity." *Frontiers in Neural Circuits* 7 (November): 181. https://doi.org/10.3389/fncir.2013.00181.

Rozzi, Stefano, Pier Francesco Ferrari, Luca Bonini, Giacomo Rizzolatti, and Leonardo Fogassi. 2008. "Functional Organization of Inferior Parietal Lobule Convexity in the Macaque Monkey: Electrophysiological Characterization of Motor, Sensory and Mirror Responses and Their Correlation with Cytoarchitectonic Areas." *European Journal of Neuroscience* 28 (8): 1569–88. https://doi.org/doi:10.1111/j.1460-9568.2008.06395.x.

Sakata, Hideo, Masato Taira, Akira Murata, and Seiichiro Mine. 1995. "Neural Mechanisms of Visual Guidance of Hand Action in the Parietal Cortex of the Monkey." *Cerebral Cortex* 5 (5): 429–38. https://doi.org/10.1093/cercor/5.5.429.

Saxe, R, S Carey, and N Kanwisher. 2004. "Understanding Other Minds: Linking Developmental Psychology and Functional Neuroimaging." *Annual Review of Psychology* 55 (1): 87–124. https://doi.org/10.1146/annurev.psych.55.090902.142044.

Schaffelhofer, Stefan, and Hansjörg Scherberger. 2016. "Object Vision to Hand Action in Macaque Parietal, Premotor, and Motor Cortices." *ELife* 5 (July): e15278. https://doi.org/10.7554/eLife.15278.

Schwartzkroin, Philip A, and Dennis D Kunkel. 1985. "Morphology of Identified Interneurons in the CA1 Regions of Guinea Pig Hippocampus." *Journal of Comparative Neurology* 232 (2): 205–18. https://doi.org/10.1002/cne.902320206.

Shepherd, Stephen V, Jeffrey T Klein, Robert O Deaner, and Michael L Platt. 2009. "Mirroring of Attention by Neurons in Macaque Parietal Cortex." *Proceedings of the National Academy of Sciences* 106 (23): 9489 LP – 9494. https://doi.org/10.1073/pnas.0900419106.

Shin, SooYoon, and Marc A Sommer. 2012. "Division of Labor in Frontal Eye Field Neurons during Presaccadic Remapping of Visual Receptive Fields." *Journal of Neurophysiology* 108 (8): 2144–59. https://doi.org/10.1152/jn.00204.2012.

Shipp, Stewart, Rick A Adams, and Karl J Friston. 2013. "Reflections on Agranular Architecture: Predictive Coding in the Motor Cortex." *Trends in Neurosciences* 36 (12): 706–16. https://doi.org/10.1016/j.tins.2013.09.004.

Song, Joo Hyun, and Robert M. McPeek. 2010. “Roles of Narrow- and Broad-Spiking Dorsal Premotor Area Neurons in Reach Target Selection and Movement Production.” *Journal of Neurophysiology* 103 (4): 2124–38. https://doi.org/10.1152/jn.00238.2009.

Taira, M, S Mine, A P Georgopoulos, A Murata, and H Sakata. 1990. “Parietal Cortex Neurons of the Monkey Related to the Visual Guidance of Hand Movement.” *Experimental Brain Research* 83 (1): 29–36. https://doi.org/10.1007/BF00232190.

Tanji, Jun. 2001. “Sequential Organization of Multiple Movements: Involvement of Cortical Motor Areas.” *Annual Review of Neuroscience* 24 (1): 631–51. https://doi.org/10.1146/annurev.neuro.24.1.631.

Thiele, Alexander, Christian Brandt, Miguel Dasilva, Sascha Gotthardt, Daniel Chicharro, Stefano Panzeri, and Claudia Distler. 2016. “Attention Induced Gain Stabilization in Broad and Narrow- Spiking Cells in the Frontal Eye-Field of Macaque Monkeys.” *Journal of Neuroscience* 36 (29): 7601–12. https://doi.org/10.1523/JNEUROSCI.0872-16.2016.

Tkach, Dennis, Jacob Reimer, and Nicholas G Hatsopoulos. 2007. “Congruent Activity during Action and Action Observation in Motor Cortex.” *The Journal of Neuroscience : The Official Journal of the Society for Neuroscience* 27 (48): 13241—13250. https://doi.org/10.1523/jneurosci.2895-07.2007.

Torres-Gomez, Santiago, Jackson D Blonde, Diego Mendoza-Halliday, Eric Kuebler, Michelle Everest, Xiao Jing Wang, Wataru Inoue, Michael O Poulter, and Julio Martinez-Trujillo. 2020. “Changes in the Proportion of Inhibitory Interneuron Types from Sensory to Executive Areas of the Primate Neocortex: Implications for the Origins of Working Memory Representations.” *Cerebral Cortex*, 1–19. https://doi.org/10.1093/cercor/bhaa056.

Trainito, Caterina, Constantin von Nicolai, Earl K Miller, and Markus Siegel. 2019. “Extracellular Spike Waveform Dissociates Four Functionally Distinct Cell Classes in Primate Cortex.” *Current Biology* 29 (18): 2973-2982.e5. https://doi.org/https://doi.org/10.1016/j.cub.2019.07.051.

Umiltà, M A, E Kohler, V Gallese, L Fogassi, L Fadiga, C Keysers, and G Rizzolatti. 2001. “I Know What You Are Doing: A Neurophysiological Study.” *Neuron* 31 (1): 155–65. https://doi.org/https://doi.org/10.1016/S0896-6273(01)00337-3.

Vigneswaran, Ganesh, Alexander Kraskov, and Roger N. Lemon. 2011. “Large Identified Pyramidal Cells in Macaque Motor and Premotor Cortex Exhibit ‘Thin Spikes’: Implications for Cell Type Classification.” *Journal of Neuroscience* 31 (40): 14235–42. https://doi.org/10.1523/JNEUROSCI.3142-11.2011.

Vigneswaran, Ganesh, Roland Philipp, Roger N. Lemon, and Alexander Kraskov. 2013. “M1 Corticospinal Mirror Neurons and Their Role in Movement Suppression during Action Observation.” *Current Biology* 23 (3): 236–43. https://doi.org/10.1016/j.cub.2012.12.006.

Wilson, F. 1994. “Functional Synergism Between Putative .” *Proceedings of the National Academy of Sciences* 91 (9): 4009–13. https://doi.org/10.1073/pnas.91.9.4009.

Yoshida, Kyoko, Nobuhito Saito, Atsushi Iriki, and Masaki Isoda. 2011. “Representation of Others’ Action by Neurons in Monkey Medial Frontal Cortex.” *Current Biology* 21 (3): 249–53. https://doi.org/https://doi.org/10.1016/j.cub.2011.01.004.

Zaitsev, Aleksey V, Nadezhda V Povysheva, Guillermo Gonzalez-Burgos, Diana Rotaru, Kenneth N Fish, Leonid S Krimer, and David A Lewis. 2009. “Interneuron Diversity in Layers 2–3 of Monkey Prefrontal Cortex.” *Cerebral Cortex* 19 (7): 1597–1615. https://doi.org/10.1093/cercor/bhn198.

Zhang, Yingying, Shasha Li, Danqing Jiang, and Aihua Chen. 2018. “Response Properties of Interneurons and Pyramidal Neurons in Macaque MSTD and VPS Areas during Self-Motion.” *Frontiers in Neural Circuits* 12 (November): 1–16. https://doi.org/10.3389/fncir.2018.00105.